Department of Civil and Environmental Engineering

Durability of Ring-Road II asphalt pavement

Phase I report on forensic analysis of Ring-Road II pavement distresses

**Terhi Pellinen, Michalina Makowska,
Pablo Olmos Martinez, Olli-Ville Laukkanen**

Aalto University | SCIENCE + TECHNOLOGY | RESEARCH REPORT

Aalto University publication series
SCIENCE + **TECHNOLOGY** 18/2013

Durability of Ring-Road II asphalt pavement

Phase I report on forensic analysis of Ring-Road II pavement distresses

**Terhi Pellinen, Michalina Makowska,
Pablo Olmos Martinez, Olli-Ville Laukkanen**

Aalto University
School of Engineering
Department of Civil and Environmental Engineering
Highway Engineering

Aalto University publication series
SCIENCE + **TECHNOLOGY** 18/2013

ISBN 978-952-60-5265-6 (pdf)
ISSN-L 1799-4896
ISSN 1799-4896 (printed)
ISSN 1799-490X (pdf)
http://urn.fi/URN:ISBN:978-952-60-5265-6

Unigrafia Oy
Helsinki 2013

Finland

Author
Terhi Pellinen, Michalina Makowska, Pablo Olmos Martinez, Olli-Ville Laukkanen

Name of the publication
Durability of Ring-Road II asphalt pavement.
Phase I report on forensic analysis of Ring-Road II pavement distresses

Publisher School of Engineering

Unit Department of Civil and Environmental Engineering

Series Aalto University publication series SCIENCE + TECHNOLOGY 18/2013

Field of research Highway Engineering

Abstract

This report presents findings from prematurely failed pavement of Ring-Road II (Kehä II) in Espoo, Finland. The road had excessive potholes, cracking, raveling and stripping only five years after construction. Core samples taken for this study revealed also that pavement layers were partially separated due to the lack of bonding. Research focus was to determine the causes of Stone Mastic Asphalt surface layer failure. Documentation of mix design, construction and material quality analysis, prior to and after construction, was compared to the samples collected from the road. Traditional quality assessment of the pavement by means of binder content and aggregate gradation analysis, air voids content, Indirect Tensile Strength and Stiffness, as well as binder tests including Penetration, Ring and Ball Softening Point and rheological characterization by Dynamic Shear Rheometer (DSR) were performed. Discrepancy was found in filler composition and additional analysis was made by applying standard analytical procedure of hydrochloric acid solubility. The findings were confirmed by means of Thermogravimetral Analysis (TGA), X-Ray Diffraction (XRD), and Scanning Electron Microscopy (SEM), supported by BET-adsorption surface area measurements. The investigation revealed presence of fly ash that was apparently used for extending limestone filler during construction. It can be concluded that the main reason for the pavement failure was due to this substitution and the consequent problems that followed in the construction and thereafter in the pavement performance.

Keywords asphalt, forensic, distress, durability, fly ash, air voids, hydrochloric acid solubility, TGA, SEM

ISBN (printed) **ISBN (pdf)** 978-952-60-5265-6

ISSN-L 1799-4896 **ISSN (printed)** 1799-4896 **ISSN (pdf)** 1799-490X

Location of publisher Helsinki **Location of printing** **Year** 2013

Pages 4+62 **urn** http://urn.fi/URN:ISBN:978-952-60-5265-6

TABLE OF CONTENTS

TABLE OF CONTENTS 5
GLOSSARY OF ACRONYMS 6
FOREWORD 7
1 INTRODUCTION 8
2 SAMPLING, VISUAL INSPECTION AND X-RAY SCANNING 11
2.1 Sampling plan 11
2.2 Visual inspection of cores and core locations 11
2.3 X-Ray Tomography 13
3 FORENSIC TESTING METHODOLOGY 16
4 RESULTS FOR CONVENTIONAL QC/QA ASSESSMENT 17
4.1 Layer thicknesses from cores 17
4.2 Mechanical properties and pavement density 19
4.3 Paving work air temperatures 23
4.4 Mixture composition and conformance to design properties 23
5 BITUMEN PROPERTIES 25
5.1 Conventional properties and DSR results 25
5.2 SARA Fractions 27
6 ADVANCED AGGREGATE AND FILLER PROPERTIES 28
6.1 Test on Solubility in hydrochloric acid (HAST) 28
6.2 Thermogravimetral Analysis (TGA) and Differential Thermal Analysis (DTA) 29
6.3 X-Ray Diffraction (XRD) 30
6.4 Surface area (SA) analysis 31
6.5 Scanning Electron Microscopy (SEM) 32
7 DISCUSSION 33
7.1 Pavement distresses vs. mechanical properties 33
7.2 Proposed pavement durability distress mechanism 36
7.3 Filler Substitution 37
8 CONCLUSIONS 37
REFERENCES 39
Appendix A: Core locations and test results 41
Appendix B: Meteorological information 59
Appendix C: Copies of construction records. 60

GLOSSARY OF ACRONYMS

ABK	Base layer asphalt concrete (kantavan kerroksen asfalttibetoni)
BET	Brunauer-Emmet-Teller -method for determining surface area
ΔR&B	Delta Ring and Ball – difference in two Softening Point readings
DOR	Density on Run, Nuclear Density Gauge
DSR	Dynamic Shear Rheometer
DTA	Differential Thermal Analysis
FA	Fly Ash
HAST	Hydrochloric Acid Solubility Test
ITSR	Indirect Tensile Strength
ITS	Indirect Tensile Stiffness
KaM	Crushed aggregate (Kalliomurske)
KTH	KTH Royal Institute of Technology (Kungliga Tekniska Högskolan)
LO	Blasted rock (Louhe)
LOI	Loss of Ignition
LTA	Paving method laying a constant thickness asphalt layer (Laatta)
NDT	Non-Destructive Testing
QC/QA	Quality Control / Quality Assurance
REM	Hot in-place remix paving method
SA	Surface Area
SARA	Saturates, Asphaltenes, Resins, Aromatics- analysis of hydrocarbon material composition
SEM	Scanning Electron Microscopy
SMA	Stone Mastic Asphalt
TGA	Thermogravimetral Analysis
TLC	Thin Layer Chromatography
UREM	Hot in-place remix paving applied to rut depths on wheel paths
VFA	Voids Filled with Asphalt
VMA	Voids in Mineral Aggregate
XRD	X-Ray Diffraction
X-Ray CT	X-Ray Computerized Tomography

FOREWORD

This report presents findings from forensic study on Ring-Road II (hereafter referred to by its Finnish name: Kehä II) asphalt pavement deterioration commissioned by the Finnish Transport Agency in 2011. The research is divided into two phases; the first phase, reported here, discusses findings from conventional quality assurance methods supplemented with advanced chemical analysis techniques. The second phase of the study will investigate more thoroughly the mineral fillers used in asphalt mixtures to develop guidelines for production quality control at asphalt plants. Also binder and mastic aging will be analyzed further.

Authors wish to acknowledge the help of Dr. Alvaro Guarin from the KTH Swedish Royal Institute of Technology in X-Ray CT Scanning of pavement cores. Authors also wish to thank following persons at Aalto University for their help in coring samples, conducting measurements and organizing work in the laboratory: Technicians Ms. Heli Nikiforow and Mr. Petri Peltonen, teaching researcher Dr. Jarkko Valtonen, and students Mr. Esko Laiho and Ms. Ute Ehlers. Furthermore, authors would like to thank Water and Wastewater Engineering Group for sharing their laboratory premises, necessary for conduction of the experiments.

Technical and financial support from Pavement Engineer MSc. Katri Eskola from the Finnish Transport Agency is also greatly appreciated.

1 INTRODUCTION

Kehä II is an important two-lane arterial road located in metropolitan area of Helsinki. The investigated road section is 6,8 km long and has ca. 49 000 vehicles/day of which ca. 2000 are heavy vehicles. The speed limit on the road is 80 km/h. Due to large areas of patching, road suffered from poor ride quality before overlay rehabilitation in 2011, see Figure1.

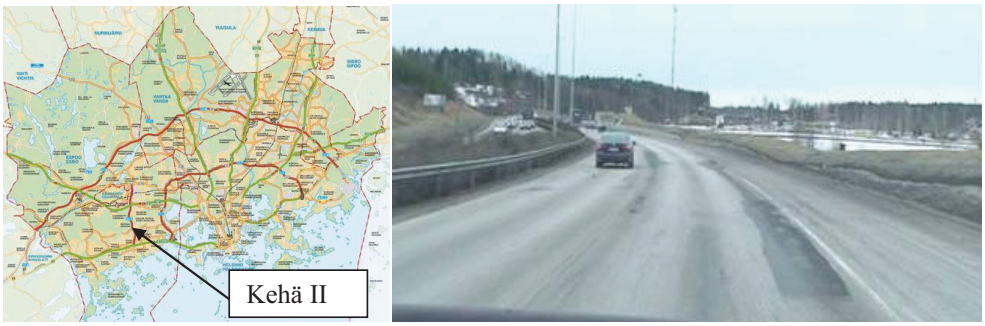

Figure 1. *Ring-road Kehä II location and pavement condition before overlay in 2011.*

Forensic investigation comprised of road condition measurements, distress inventories, analysis of construction and maintenance records and laboratory testing. Sampling, majority of laboratory testing, and data analysis have been conducted by Aalto University Transportation research group. Investigations listed below have been conducted and are discussed in this report.

- Review of initial pavement design and mix design records and QC/QA reports of subsequent paving work and review of rehabilitation paving work records
- Videotaping and visual inspection of road
- Sampling and photographing samples
  - 50 cores and two slab samples were taken
- Laboratory testing
  - Conventional quality assurance (QA) testing
  - Rheological binder testing using Dynamic Shear Rheometer (DSR)
  - Chemical analysis techniques
- X-Ray CT scanning of selected cores by KTH (Sweden)

Pavement condition was measured on 24-26.4.2011 at night by Roadscanners Oy. A separate report ”Nykytilaselvitys 2011, Kehä II välillä Länsiväylä-Turuntie” is available.

The ring-road Kehä II was constructed in two stages; the entire construction history is shown in Figure 2. Stage I construction was completed in year 2000. Pavement thickness design included 700-mm thick rock bed base course of blasted rock (LO) over 250-mm thick crushed rock (KaM) layer. The bound base course was 70-mm thick asphalt concrete base layer (ABK), and at top of that was 40-mm thick binder course layer of SMA20 (*Pihlajamäki and Sikiö* 2001). The SMA 20 binder course was used as a wearing course for two years before completing the road construction for the designed structural thickness. In Stage II construction, 40-mm thick wearing course of SMA 16 (LTA) was placed down in autumn 2002, see Figure 2.

Despite predictions of good performance over 20 years of design life, distresses such as potholes, cracking and raveling started to emerge. Sections of the road surface were rehabilitated using hot in-place Remix technique in 2007, 2008 and 2009 mixing 16 to 19 kg/m^2 fresh SMA 16 with existing SMA 16 mixture. The multiple attempts of surface rehabilitation were ineffective and, in 2011, road was overlaid with 40-mm thick SMA 16 layer. The Remix treatment was applied only partially for the most deteriorated road sections and Figure 4 show the locations of road where the Remix rehabilitation was applied. Map also shows the locations were cores were taken for laboratory testing.

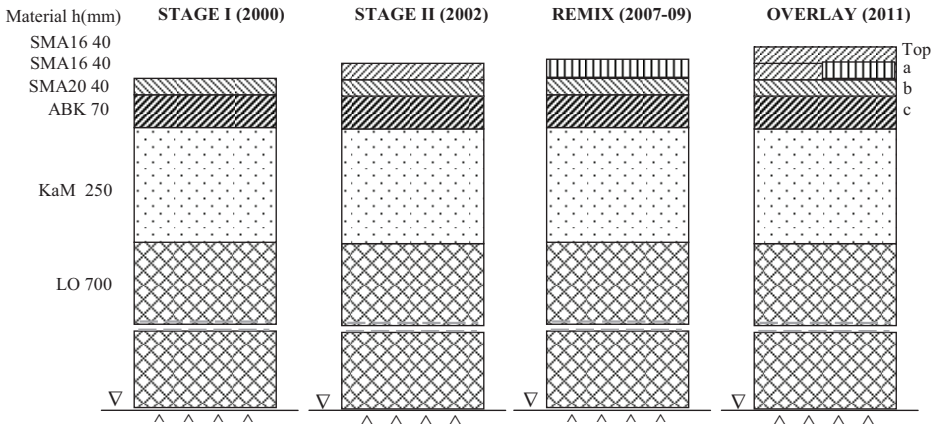

Figure 2. *Kehä II construction history: pavement structural design. Layers are designated as follows: Top is the new SMA16 overlay, (a) is Stage II original binder course layer with or without rehabilitation, (b) is binder layer SMA20, and (c) is ABK layer.*

In recent years, maintenance and recycling of old asphalt pavements have become a major activity in road construction. Among European countries, Finland is leading in the use of in-place hot-mix recycling techniques shown in Figure 3, and its use is steadily increasing as government funding for pavement repairs and overlaying has declined. As the added new material is usually less than 20 kg/m2, the structural capacity of road is not increasing. Based on research project conducted by *Apilo and Eskola* (1999) a country wide decision was made to allow same road to be rehabilitated only twice before applying new overlay.

Figure 3. *Hot in-place recycling: heating, milling and addition of new fresh mixture.*

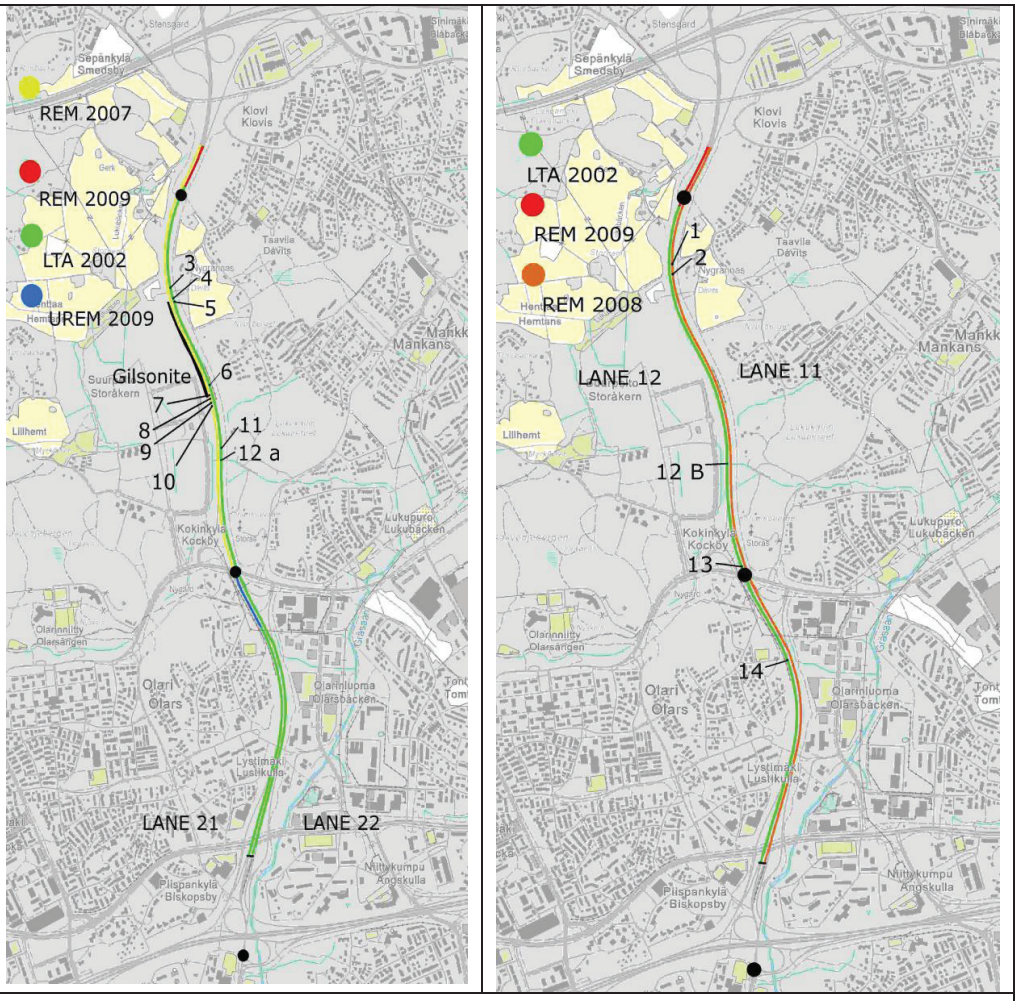

Figure contains data from the National Land Survey of Finland Topographic Database 08/2012.

	1.1	1.2	2.1	2.2	North
1	N				
2	M				
3				C	
4				B	
5				A	
6				D	
7			J		
8			I		
9			H		
10			G		
11				F	
12 a				E	
12 b		O			
13		L			
14		K			South

Figure 4. *A map of road for Remix (REM) and Stage II (LTA) sections (Tierekisteri).*

2 SAMPLING, VISUAL INSPECTION AND X-RAY SCANNING

2.1 Sampling plan

In May 2011, before the new overlay was laid, 50 cores were taken from 15 locations, as shown in Table 1. Based on visual inspection, samples were selected to be taken from "bad" and "good" areas of road, bad areas containing potholes, patches and ravelling. Road condition was videotaped before coring and a map of cores was sketched during coring, see Figure 5. Additional samples were taken in January 2012 from locations E and O after the new surface layer had been laid. These new samples were pavement slabs. A detailed log of the samples is presented in Appendix A.

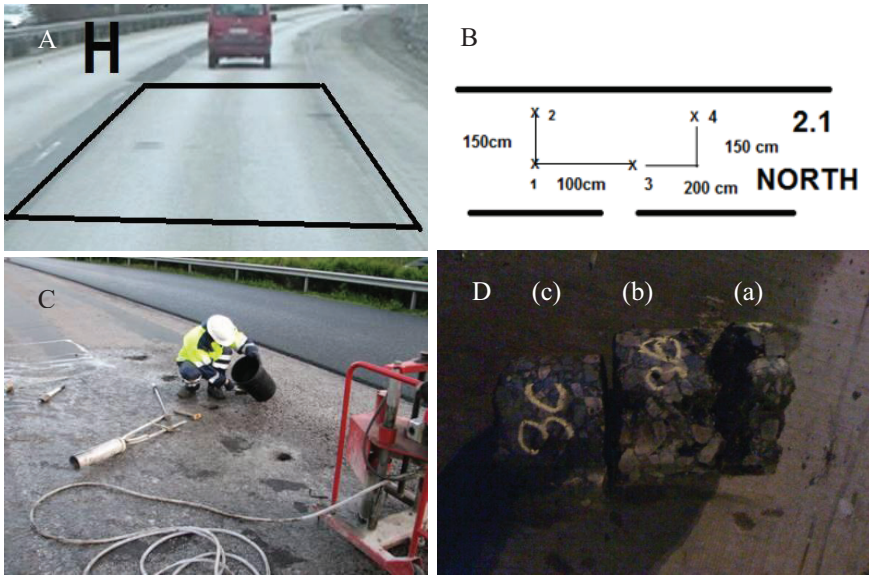

Figure 5. *A) Core location H, B) coring plan, C) obtaining samples by coring, D) pavement layers separated during coring, layer (a) is wearing course, (b) is binder course SMA 20 and layer (c) is asphalt base course (ABK) .*

2.2 Visual inspection of cores and core locations

Table 2 shows results of visual inspection of cores and pavement condition in core location. Visual observation of cores showed layer separation, loss of binder, pumping of water through surface layer, cracking and raveling. Visual inspection of road at core locations revealed raveling, patching and potholes.

Table 1. *Sampling scheme and core locations. Distances are matched to the readings reported by Roadscanners Oy (Location/distance).*

Direction /lane	Surface layer		Location/ distance (m)		Qty of cores	Notes
NBDL 1.1	SMA 16 REMIX 2008	M	osa 2	1486	5	Surface in good condition but separated from layer b
		N	osa 2	1529	5	
NBPL 1.2	SMA 16 LTA 2002	K	osa 1	1548	5	K is in good condition, L is bad as all layers are separated
		L	osa 2	21	7	
	SMA 16 LTA 2011	O	osa 2	517	1 slab	Core was drilled in lab
SBDL 2.1	SMA 16 REMIX 2007	G	osa 2	805	2	In good condition, full samples obtained, layers were bonded expect layer H which was in bad condition
		H	osa 2	815	4	
		I	osa 2	828	2	
		J	osa 2	838	1	
SBPL 2.2	SMA 16 LTA 2002	A	osa 2	1342	2	Generally in bad condition, samples broke during coring and layers were not bonded except in location D
		B	osa 2	1362	3	
		C	osa 2	1414	3	
		D	osa 2	911	3	
		E	osa 2	557	4	
		F	osa 2	607	4	
	SMA 16 LTA 2011	E	osa 2	557	1 slab	

NBDL = North bound driving lane, NBPL = North bound passing lane, SBDL = South bound driving lane, SBPL = South bound passing lane.

Table 2. *Visual observations of road distresses.*

Core location	Surface layer age (years)*	Visual observation of surface condition	Visual observations from cores			
			layers bonded		Moisture pumping	Broken samples
			a-b	b-c		
A,B,C	9	deteriorated	no	**	yes	yes
D	9	quite good	yes	no	yes	no
E,F	9	deteriorated	no	**	yes	yes
G,J	4 (REM)	good	yes	yes	no	no
H	4 (REM)	deteriorated	no	no	yes	yes
I	4 (REM)	good	yes	yes	no	no
K	9	good	yes	yes	no	no
L	9	deteriorated	no	no	yes	yes
M	3 (REM)	deteriorated	yes	no	no	no
N	3 (REM)	good	yes	no	no	no
O	0 (REM)	good	yes	yes	no	no

*Age of wearing course surface layer before 2011 overlay.
** Cores broke and only surface layer was retrieved

Initial findings during sampling suggested very weak pavement structure as cores broke during coring, see Figure 6. In location O, there was some finer levelling course mixture placed between the ABK and SMA 16 binder course layers, as shown in Figure 7a. Visual inspection of pavement slabs confirmed that the original SMA 16 2002 layer was brittle and colour of asphalt was brown while the newly laid SMA layer was black and shiny as expected (Figure 7b). Also, there was thin layer of ice underneath the SMA 16 LTA 2002 layer indicating that moisture was able to infiltrate to the pavement structure due to lack of bonding between layers.

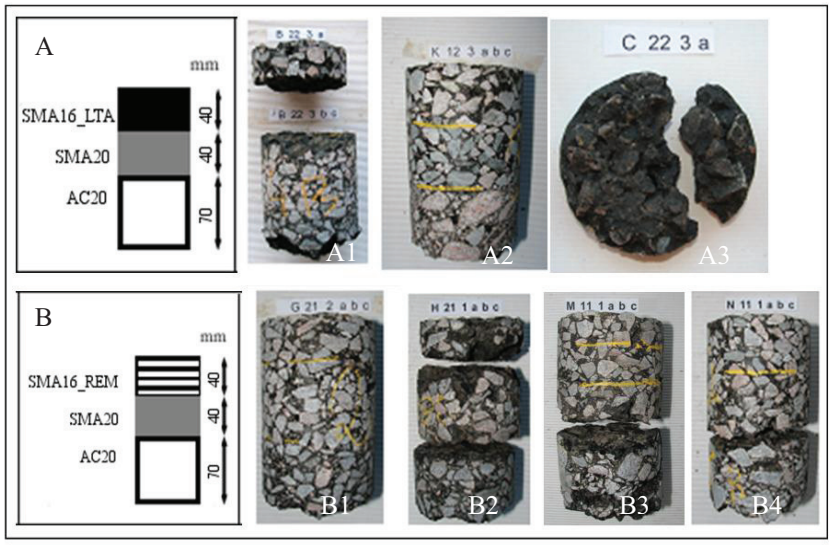

Figure 6. *(A) Sketch of original road structure asphalt layers – 2002, (A1) surface layer was not bonded; (A2) monolithic pavement structure in good condition; (A3) weak mixture and binder washed away; (B) sketch of road structure after rehabilitation in 2007-09, (B1) structure in good condition; (B2) all layers were separated; (B3&B4) ABK layer is separated.*

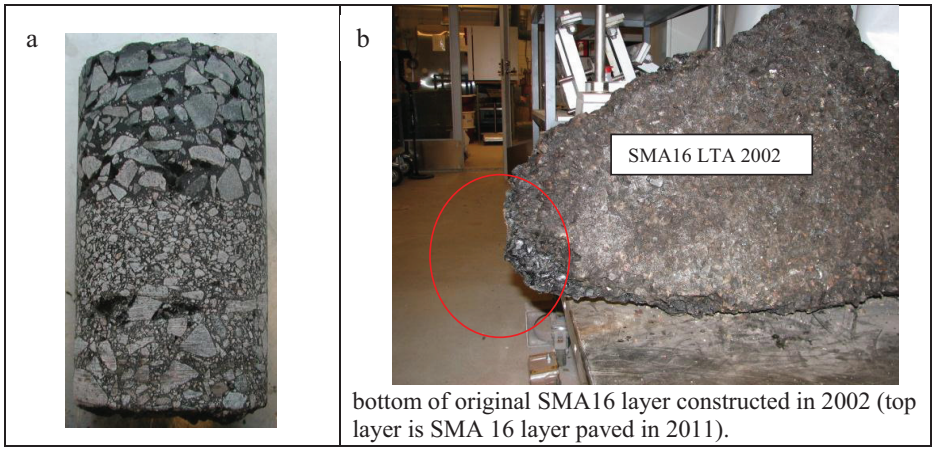

bottom of original SMA16 layer constructed in 2002 (top layer is SMA 16 layer paved in 2011).

Figure 7. *a) Core drilled from location O, b) slab from location E, brown color of SMA 16 LTA 2002 is clearly visible.*

2.3 X-Ray Tomography

Four samples – one from each of the locations H, I, M and N – were sent to KTH for X-ray scanning. All samples were from areas rehabilitated with Remix technique representing relatively good pavement condition. The X-Ray Computerized Tomography (X-Ray CT) is a non-destructive technique which allows us to visualize the interior of cores by capturing digital information on core's 3-D microstructure. According to Farcas (2012) "X-Ray CT consists generally of an X-Ray source, a detector, and a turntable carrying the test specimen

in between the source and the detector. X-Ray intensities are measured before and after they are emitted through the specimen in different directions for a full rotation of the specimen. The intensity values are used for calculating the distribution of the linear attenuation coefficient in order to generate a map representing the density at every point of the test specimen". The KTH X-Ray scanner is shown in Figure 8.

Figure 8. *X-Ray CT Scanning Machine at KTH.*

Figures 9 to 12 show the test specimen photographs and tomography pictures for the whole core and three slices from top, middle and bottom of core. It can be seen from the figures that there were large air void pockets in the specimens. Photos from samples H, I and N show black continuous lines between layers indicating that layers are not well bonded and there is a small gap between them. In sample M, joints are not visible but the whole sample has large air void pockets. These photos suggest that the treated or remixed layer depth was less than 40 mm for all other samples expect for perhaps sample M.

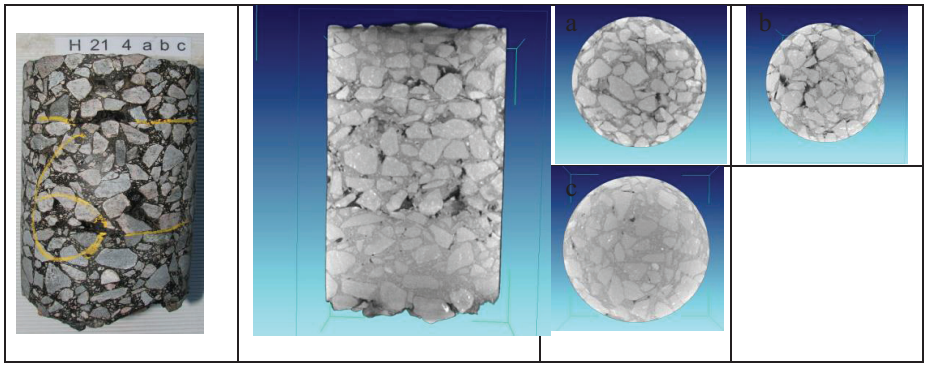

Figure 9. *X-Ray scan of core H 21 4abc, on right: top (a), middle (b) and bottom (c) slice of the core.*

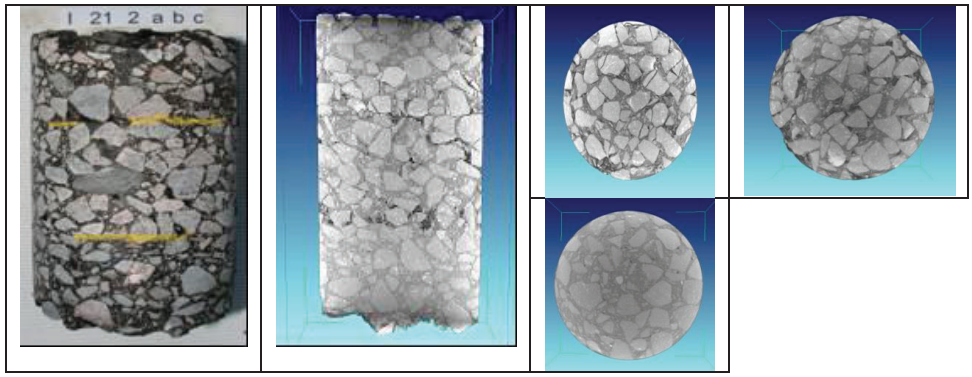

Figure 10. *X-Ray scan of core I 21 2abc, on right: top, middle and bottom slice of the core.*

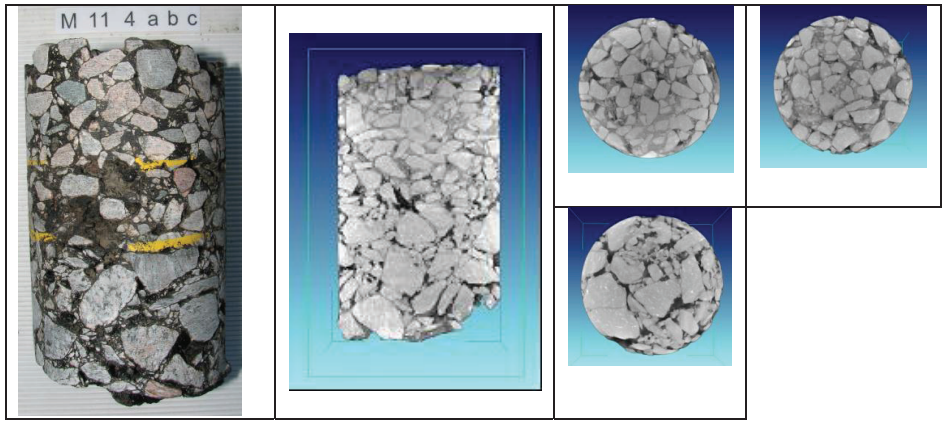

Figure 11. *X-Ray scan of core M 11 4abc, on right: top, middle and bottom slice of the core.*

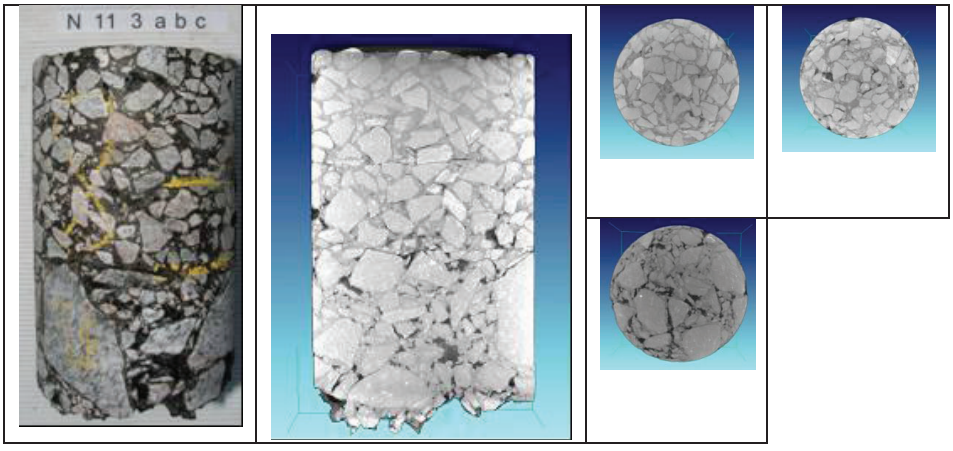

Figure 12. *X-Ray scan of core N 11 3abc, on right: top, middle and bottom slice of the core.*

3 FORENSIC TESTING METHODOLOGY

Laboratory testing concentrated on layer (a) shown in Figure 2, which seemed to be the most damaged layer. Some additional testing on layers (Top), (b) and (c) was also conducted.

Core samples were separated into layers either by means of self-detachment (bad samples) or cutting by diamond saw (good samples), see Table 3. Mechanical and chemical tests were performed to explain differences between "good" and "bad" pavement locations. Tests included conventional QA testing, more advanced rheological testing for binders and chemical analysis for fillers separated from extracted aggregate. Indirect tensile stiffness and strength measurements could not be conducted on samples collected from very bad locations mostly due to the fact that samples were so weak that they were falling apart during handling. Bulk density measurements were conducted in two ways, either separating all layers or testing entire core.

Table 3. *Testing plan: (C) is core, (LM) is loose mixture and (EM) is extracted material from loose mixture.*

Testing type	Test method	C	LM	EM	Notes
Conventional QA testing	Layer thickness	x			All samples
	Bulk density SSD	x			All samples
	IT stiffness and strength	x			Partial testing, worst samples not tested.
	Maximum density		x		All locations layer (a), some (b) and (c).
	Bitumen content	.		x	AB, C, E, G, I, J, K
	Gradation			x	AB, C, E, G, J
	Aggregate & filler density			x	AB, C, K
	Penetration, Softening point			x	AB, C, E, G, I, J
	Fraass breaking point			x	AB, C, E, G, J
Rheology	DSR testing for bitumen			x	AB, C, E, G, J, L
Chemical analysis	Bitumen SARA fractions			x	C, E, G
	Filler surface area			x	AB, C, K
	Solubility in hydrochloric acid			x	C, E, G, O
	TGA			x	E, G
	XRD			x	E, G,
	SEM			x	E, G

All samples were then subjected to the measurement of bulk density (EN 12697-6, method A and B). The maximum density of mixture (EN 12697-5) of each sampling location was obtained by combining material from the same layers of several cores to obtain large enough specimens for testing. On the basis of the above results, air voids content was calculated, according to EN 12697-8.

Samples were processed according to EN 12697-1; methyl chloride was used as an extracting solvent. Bitumen was recovered by rotary evaporation method according to EN 12697-3 and bitumen content was calculated according to EN 12697-1. Centrifugation did not reveal any residue and investigation of binder by means of optical spectroscopy did not reveal any solid cluster formations. Additional binder content testing by thermal decomposition (EN 12697-1:2005, Annex C) conducted on recovered binder resulted in 100 % mass loss reading in the temperature of 575 °C.

Extracted binder was investigated by means of Penetration (EN 1426), Ring and Ball Softening Point (EN 1427) and Fraass breaking point (SFS-EN 12593:2007) tests. Further

analysis of binder was conducted by separation into SARA fractions and conducting rheological investigation using Dynamic Shear Rheometer (DSR).

Aggregate and filler densities were measured according to SFS EN-1097-3 and SFS EN-1097-4, respectively. Aggregate particle size distribution was determined according to EN 933-2. Each size fraction was retained separately and representative samples were further studied by TGA, XRD, SEM and hydrochloric acid solubility tests (PANK 2405). Additionally, filler surface area was determined according to DIN 66131 (PANK 2401) at University of Turku. Results from aforementioned tests are shown in Appendix A.

4 RESULTS FOR CONVENTIONAL QC/QA ASSESSMENT

4.1 Layer thicknesses from cores

Figures 13 to 16 show the measured thicknesses of pavement layers in each lane of Kehä II. For some samples it was difficult to see the layer boundaries (locations M and N) but for many samples it was easy as layers were not bonded together. Visual inspection suggested that locations with thin wearing course layer had more distresses and potholes.

Southbound passing lane was badly deteriorated as cores broke, and therefore full depth cores were not obtained from most of these locations (Figure 16). Northbound lanes were in better condition and total pavement thickness generally met or exceeded the total design thickness of 150 mm (70+40+40 mm). This agrees with construction records, as the amount of laid mixture was reported to be 99,06 - 99,93 kg/m^2, i.e., layer thickness being 40 mm. However, construction records did not indicate how much tack coat (glue) in liters was used during construction. The observed bond failure between layers was caused either by lack of applying tack coat during construction, or by the fact that it was washed away by excessive water infiltration to the pavement, or by the combination of these both.

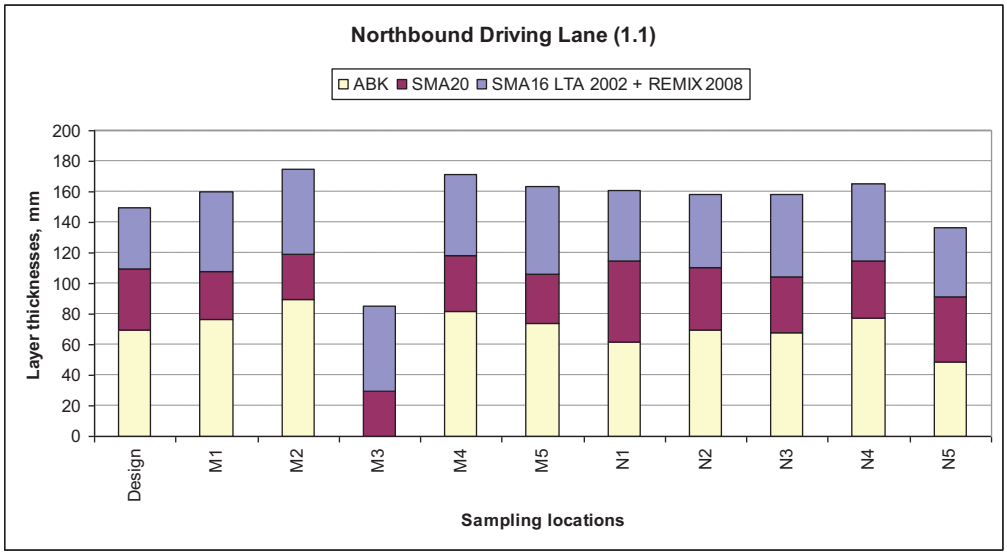

Figure 13. *Core thicknesses of northbound driving lane samples.*

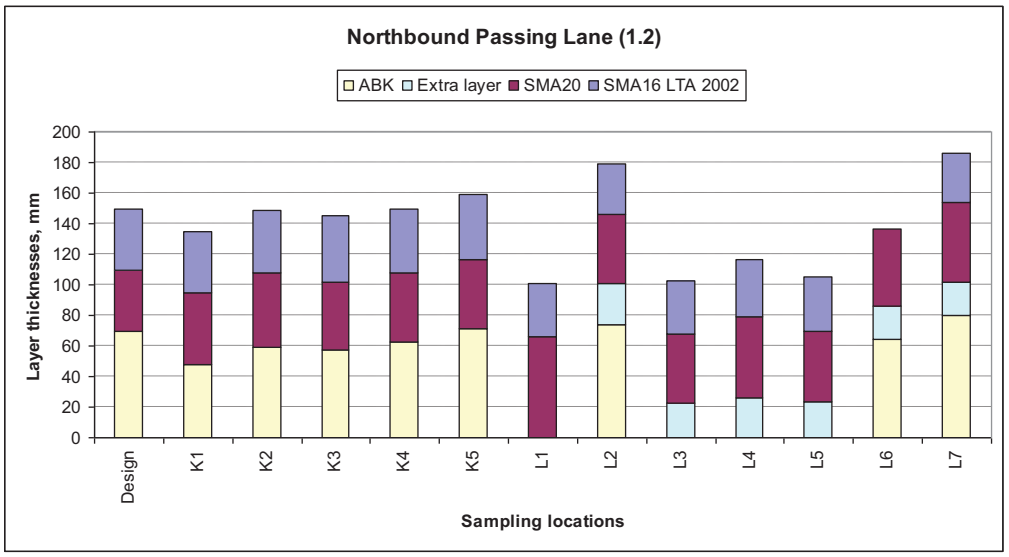

Figure 14. *Core thicknesses of northbound passing lane samples.*

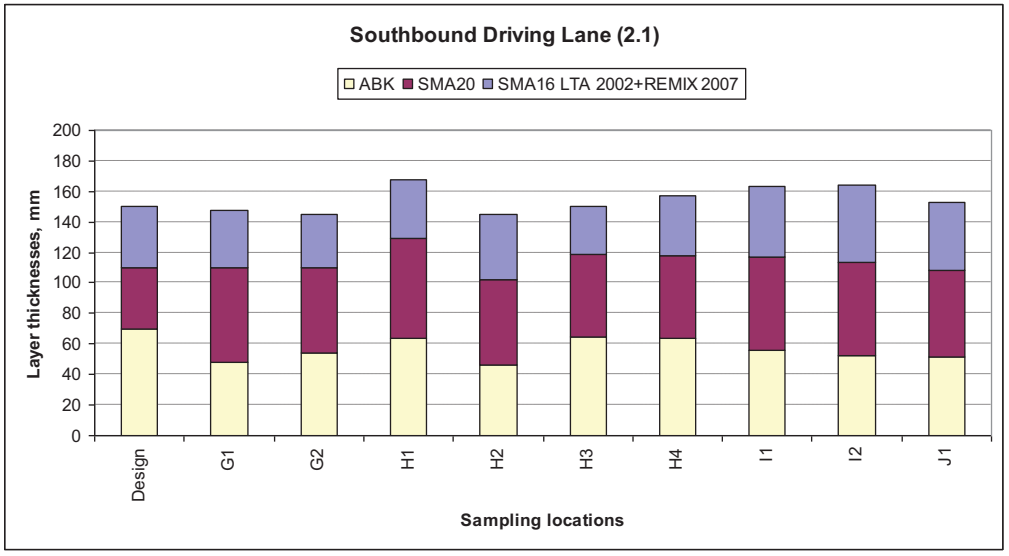

Figure 15. *Core thicknesses of southbound driving lane samples.*

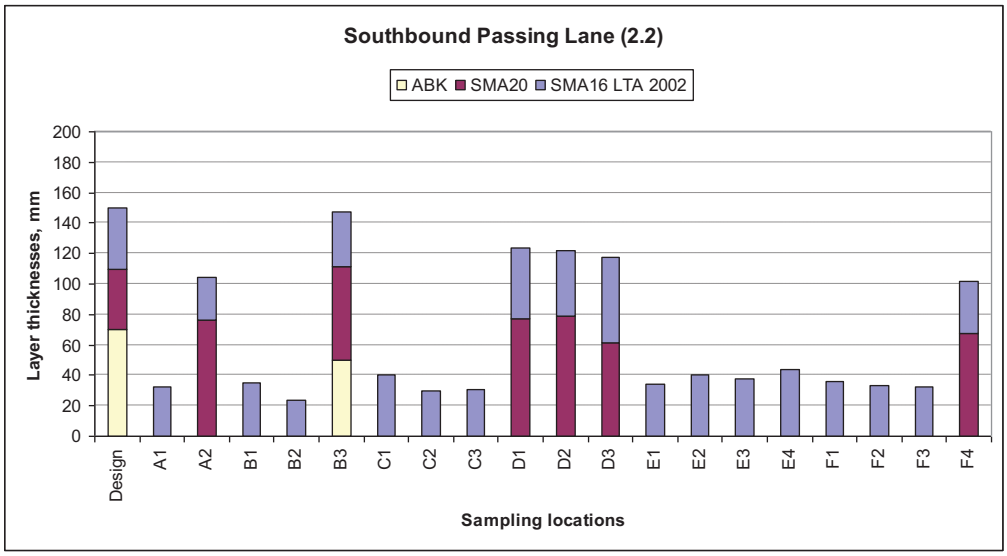

Figure 16. *Core thicknesses of southbound passing lane samples.*

4.2 Mechanical properties and pavement density

Selected set of samples were subjected to Indirect Tensile Stiffness (ITS, SFS-EN 12697-26, Annex C) and indirect Tensile Strength (ITSR, SFS-EN 12697-23) testing, see Figure 17. Stiffness was measured first at 10 ºC using 124 ms rise time and pulse repetition period of 3 seconds. Then specimen was tested for strength applying 50 mm/min loading time. Measurement could not be conducted on most samples collected from bad locations. Some of the samples were not round, some cracked during coring from the pavement, some layers detached and stayed inside the drill and had to be removed by destructive methods and some cracked due to handling during preparation (see Figure 5d and 6). Although for some samples stiffness measurements were not possible due to rocking of specimen in the loading fixture, strength testing was conducted.

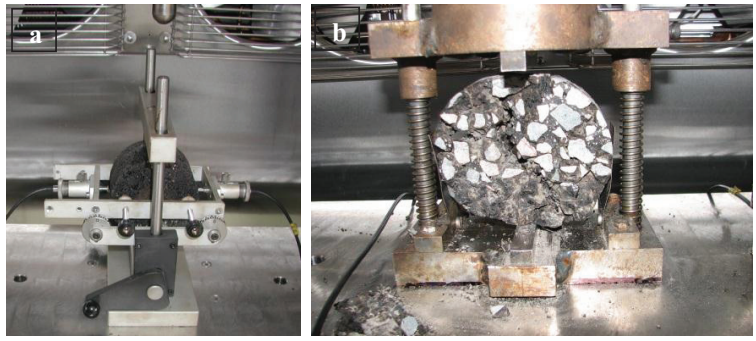

Figure 17. *Test configurations for Indirect Tensile Stiffness (a) and Strength (b).*

Tables 4, 5 and 6 summarize pavement density and mechanical properties for layers (a), (b), and (c) for each sampling location with average layer thickness measured from cores.

Table 4. *Average density, stiffness and strength for layer (a).*

Lane	Area	Mix density ρ_m, (Mg/m^3)		Bulk density ρ_b (Mg/m^3)		Air voids (%)	Thickness (mm)		Stiffness ITS (MPa)		Strength ITSR (MPa)	
		Avg.	n	Avg.	n	Avg.	Avg.	n	Avg.	n	Avg.	n
NBDL 1.1	M	2,438	1	2310	3	5,3	54,8	5	6127	3	1,86	3
	N	2443	1	2361	2	3,4	49,0	5	8933	2	2,38	2
NBPL 1.2	K	2442	2	2345	2	4,0	41,8	5	7505	2	2,10	2
	L	2451	1	2242	6	8,5	35,6	6	*		0,71	2
	O	2569	1	2489	1	3,1	40,5	1	4572	1	1,86	1
SBDL 2.1	G	2430	1	2364	2	2,7	36,2	2	6881	2	2,54	2
	H	2436	1	2286	2	6,2	38,0	4	*		0,83	1
	I	2430	1	2354	2	3,1	48,1	2	8708	1	2,56	1
	J	2441	1	2368	1	3,0	45,1	1	9115	1	2,41	1
SBPL 2.2	A	2452	1	2286	1	6,8	30,1	2	*		*	
	B	2452	1	2279	3	7,1	31,3	4	*		*	
	C	2454	1	2295	3	6,5	33,6	3	*		*	
	D	2445	1	2305	2	5,7	44,6	3	7567	2	1,73	2
	E	2437	1	2283	4	6,3	39,2	4	*		1,24	2
	F	2450	1	2306	4	5,9	34,6	4	*		1,21	2

* Not possible to test due to too weak or impaired samples.

Table 5. *Average density, stiffness and strength for layer (b).*

Lane	Area	Mix density ρ_m, (Mg/m^3)		Bulk density ρ_b (Mg/m^3)		Air voids (%)	Thickness (mm)		Stiffness ITS (MPa)		Strength ITSR (MPa)	
		Avg.	n	Avg.	n	Avg.	Avg.	n	Avg.	n	Avg.	n
NBDL 1.1	M	2,430	1	2,243	3	7,7	31,6	5	-		1,24	2
	N	2,430	1	2,268	2	6,7	42,1	5	5121	1	1,92	3
NBPL 1.2	K	2,487	1	2,456	2	1,2	46,3	5	5214	2	2,0	1
	L	2,424	1	2,276	6	6,1	51,2	7	6414	4	1,8	2
	O											
SBDL 2.1	G	2,443[a]	n/a	2,343	2	4,1	58,7	2	10341	1	*	
	H	2,443[a]	n/a	2,294	2	6,1	57,4	4	7015	1	*	
	I	2,443[a]	n/a	2,324	1	4,9	61,1	2	10596	1	*	
	J	2,443[a]	n/a	2,351	1	3,8	56,4	1	11464	1	*	
SBPL 2.2	A	2,443[a]	n/a	2,327	1	4,9	76,4	1	-		-	
	B	2,443[a]	n/a	2,408	1	2,8	61,7	1	-		-	
	C	2,443[a]	n/a	-		-	-		-		-	
	D	2,443[a]	n/a	2,372	3	2,9	70,7	3	10008	1	*	
	E	2,443[a]	n/a	-		-	-		-		-	
	F	2,443[a]	n/a	2,267	1	7,2	767,7	1	7889	1	-	

[a)] Average measured value.

* Not possible to test.

Table 6. *Average density, stiffness and strength for layer (c).*

Lane	Area	Mix density ρ_m, (Mg/m^3)		Bulk density ρ_b (Mg/m^3)		Air voids (%)	Thickness (mm)		Stiffness ITS (MPa)		Strength ITSR (MPa)	
		Avg.	n	Avg.	n	Avg.	Avg.	n	Avg.	n	Avg.	n
NBDL 1.1	M	2,347[a]	n/a	2,345	3	3,8	77,5	4	-		-	
	N	2,347[a]	n/a	2,350	3	3,6	66,2	5	-		-	
NBPL 1.2	K	2,437	n/a	2,383	2	2,2	59,6	5	18787	1	2,6	1
	L	2,490[a]	n/a	2,413	3	3,1	72,8	3	-		-	
	O	-	-	-		-	-		-		-	
SBDL 2.1	G	2,490[a]	n/a	2,449	2	1,6	51,2	2	-		-	
	H	2,490[a]	n/a	2,439	2	2,1	59,6	4	-		-	
	I	2,490[a]	n/a	2,489	1	0	54,3	2	-		-	
	J	2,490[a]	n/a	2,464	1	1,0	51,8	1	-		-	
SBPL 2.2	A	-	-	-		-	-		-		-	
	B	-	-	-		-	50,1	1	-		-	
	C	-	-	-		-	-		-		-	
	D	2,490[a]	n/a	2,454	1	1,4	61,3	1	-		-	
	E	-	-	-		-	-		-		-	
	F	-	-	-		-	-		-		-	

[a] Calculated value

A correlation was found between Indirect Tensile Strength values at 10 °C and air voids content (Figure 18), with bad areas of high air voids content giving predicted response of lower strength.

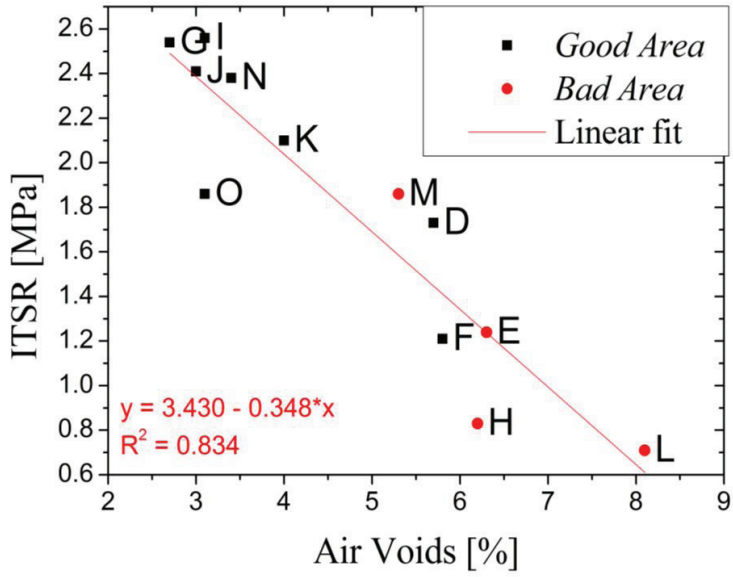

Figure 18. *Mixture Indirect Tensile Strength vs. air voids content, layer (a).*

Thickness of the surface layer was found to be between 30 and 55 mm. Figure 19 presents correlation attempt between the air voids content and the layer thickness. Generally for the original surface layer SMA 16 LTA, deteriorated "bad" areas could be characterized by low thickness and high air voids content. Sample set marked inside the dotted line represents rehabilitated areas (REM) and higher pavement thicknesses are due to the addition of fresh material during the remixing process. Analogically, it can be concluded that reheating and additional compaction has contributed to the increase of pavement density compared to the original layer.

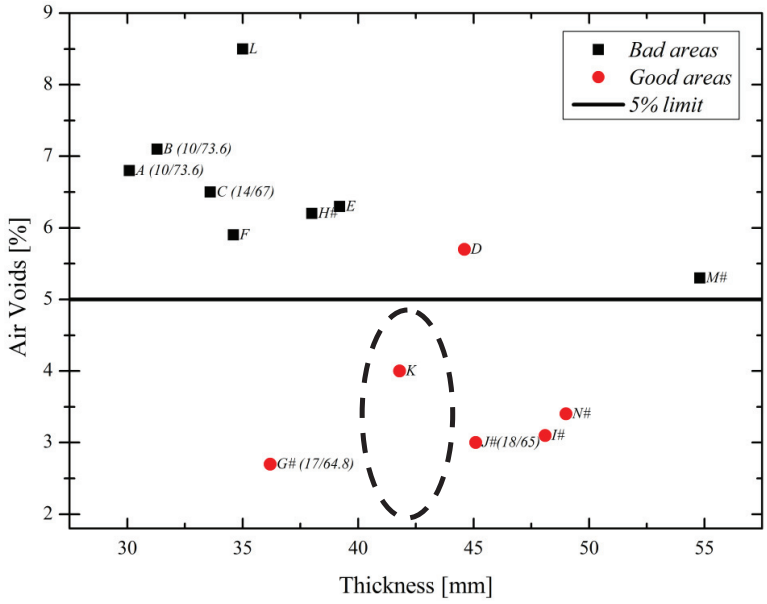

Figure 19. *Air voids content vs. thickness of layers (a). Oval region represents design values from mix design report. Hash sign (#) denotes samples from the rehabilitated area. Samples outside that are representative of original 2002 surface layer. Labels represent the area where samples were collected, followed by Penetration and Softening Point value, when available.*

It is plausible that the origin of the high air voids content in the SMA16 LTA layer is due to poor compaction of too thin asphalt layer combined with too low compaction temperature. Rule of thumb is that for proper compaction, the layer thickness should be 2,5 to 3 times the maximum aggregate size, which in this case is 40 to 48 mm. In addition, it can be speculated that poor mixture workability (discussed further in section 4.5) has also contributed to the problem.

In stage II construction, the quality control for air voids content was made using NDT testing with DOR apparatus. The average measured air voids contents (n = 4448) was reported to be 2,7 % and a the standard deviation was 2,42 %. Mix density ρ_m used in the calculations was 2456 kg/m^3. QC report (see Appendix C) also stated that the upper tolerance limit for air voids content was 6 % and only 0,08 % exceeded the limit of 6 %. Based on this report,

pavement compaction was acceptable at the time of construction. However, all the bad areas were found to have 5-8 % air voids content and layer thicknesses were less than the required minimum of 40 mm, while the good area K had air voids content of 4 % and 40-mm layer thickness.

It is not known why 6 % criterion was used for construction QC because according to the specifications (PANK 2000) criterion should be 5 %. Therefore, assuming normally distributed air voids content in the pavement, approximately 15,8 % of the DOR measurements would exceed 5 % air voids content and similar percentage of measurements would have negative air voids content. As negative values are not physically possible, it must be concluded that the air voids distribution clearly deviates from normal distribution in this case: in truth the percentage of pavement exceeding 5 % void content is very likely to be higher than 15,8 %. This discrepancy between forensic analysis and QC air voids results may be due to an error in the DOR calibration processes at the time or biased selection of sample locations during testing.

4.3 Paving work air temperatures

Construction records showed that the dates for paving work for 40-mm thick overlay were 30.9-11.10.2002. Air temperature records at Kaisaniemi (in the centre of Helsinki) obtained from Finnish Meteorological Institute can be used to estimate air temperatures during paving work. As Kaisaniemi is in the city centre, temperatures are slightly higher than in Kehä II, which is outside the city. Records show that temperature varied between -1,8 and 9,4 °C between ten o'clock in the evening and six o'clock in the morning. After first of October temperatures decreased ca. 10 °C. It is difficult to obtain proper compaction when air temperatures are so low and often higher production temperatures are used to compensate the fast cooling of mixture.

In turn, the Remix rehabilitation construction was done in June and July, when the average daily air temperatures were above 10°C, which allowed more time for compaction. However, during 2007 work, for 5 of the 6 working days the meteorological data reports show rain up to 23,7 mm and during 2008 work, 4 out of 8 days had records of rain up to 10 mm (see Appendix B).

4.4 Mixture composition and conformance to design properties

Examination of construction quality control /quality assurance (QC/QA) records for SMA 16 LTA revealed discrepancies between design and actual construction. In addition, mix design data and information of raw materials was scarce.

SMA 16 wearing course was designed to be a mixture of 3 fractions, namely sand (#0-2), gravel (#5-8) and crushed rock (#8-16) from Koskenkylä, in ratio of 15:10:66. Additionally, 9 % limestone filler from Sipoo was designed to be added, see Table 7.

Design bitumen content was selected to be 6,1 % and 0,33 % cellulose fibre (EKI-12) was to be added to prevent binder drain-down. Design bitumen grade was 70/100 (B-80). However, a cost charge was found in the documentation for SMA16 with 8 % of unspecified filler. Mixture design VMA was 17 % and VFA was 83 %, maximum density was 2447 kg/m^3 and design pavement density was 2377 kg/m^3 with design air voids content of 2,8 %. Details of design are shown in Appendix C.

Construction QC information for Kehä II was obtained from District of Uusimaa paving contract records of 2002. QC data shown in Table 7 is based on 71 samples of SMA 16 mixture from Maantiekylä asphalt plant (see Appendix C).

Table 7. *Summary of Mix Design and QC/QA results for SMA 16 LTA 2002.*

Property	**Design**	**Notes**	**QC**	
	SMA16		**Avg.**	**St.dev.**
Binder content, %	6,10		5,97	0,11
Binder grade	70/100			
Fibre amount, % of mix	0,33	type; EKI12		
Gradation				
Passing 0.063 mm %	9,9		9,9	0,51
Passing 2 mm, %	22,4		20,5	1.14
Passing 4 mm. %	27,0		22.7	1.52
Passing 8 mm,%	36,8		29,8	1.85
Passing 11.2 mm, %	59,1		56,0	3.65
Passing 16 mm, %	96,5		95,1	1.71
Aggregate proportioning				
Filler, %	9,0	ρ = 2770 kg/m^3	8,0	
Baghouse fines	0.0		1,0	
Fine sand 0-2 mm, %	15,0	ρ = 2700 kg/m^3	15,0	
Mid-size 5-8 mm, %	10,0	ρ = 2690 kg/m^3	10,0	
Coarse 8-16 mm, %	66,0	ρ = 2680 kg/m^3	66,0	
Aggr. blend density		ρ_{blend} = 2692 kg/m^3		
Max. density of loose mix		ρ_m = 2447 kg/m^3		
Pavement bulk density		ρ_b = 2377 kg/m^3		

The average binder content in QC records was 5,97 % with standard deviation of 0,11 % (Table 7). Forensic testing (Table 8) revealed that for the bad areas, the average binder content was 6,0 %, while the only truly good area (K) had binder content of 6,3 %. Amount of fines (<0,063 mm) in QC reports were well within design limits; only percent passing 4 mm was 5 % and passing 8 mm was 7 % coarser than specified, Figure 20. Our testing indicated some segregation, i.e., lower binder content corresponds to a coarser gradation.

Table 8. *Mixture composition from cores.*

Property	**AB**	**C**	**E**	**G**	**J**	**K**
Binder content, %	5,90	5,90	6,20	6,08	5,94	6,30
Gradation						
Passing 0.063 mm %	9,2	7,7	11,0	7,4	10,4	11,0
Passing 2 mm, %	22,4	21,9	24,5	24,0	25,0	
Passing 4 mm. %	24,8	23,9	26,9	27,6	27,5	
Passing 8 mm,%	33,3	32,7	35,2	42,9	39,0	
Passing 11.2 mm, %	62,7	63,8	56,4	70,8	66,0	
Passing 16 mm, %	97,8	96,2	96,2	98,7	99,0	
Filler						
Filler surface area, m^2/g	2,757	3,567	-	-	-	2,844

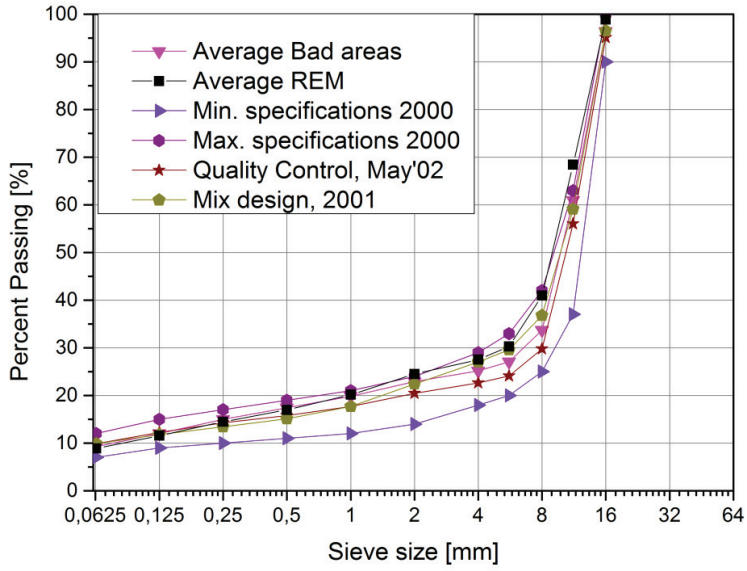

Figure 20. *Aggregate gradation curves.*

Observations: Magnetic particles were found on the walls of the extractor after binder content evaluation, in the fraction of 0,063-0,5 mm. Furthermore, after extraction fines expressed increased hydrophobicity, despite no apparent remains of methyl chloride soluble organic residue could be found. This prevented performing standard measurements of particle density of filler in water (EN 1097-7) and gradation curve of minus 0.063 mm fraction via hydrometer technique (EN 1687). Similar behavior was observed in our laboratory previously for fines of extracted samples containing fly ashes (FA) as filler.

5 BITUMEN PROPERTIES

5.1 Conventional properties and DSR results

Penetration values and Softening Point values (65-74 °C) are consistent with aged binder extracted from pavements of similar age and similar air voids content although some variation existed (*Whiteoak* 1990*,* Shell Bitumen Handbook). Based on penetration measurements and excluding reference binder 70/100, area J had the softest binder and area AB had the stiffest, see Table 9.

The Fraass breaking point test (SFS-EN 12593:2007) determines the temperature at which bitumen breaks instead of stretching when it bends. The Fraass Breaking Point is the temperature at which the first cracks appear in the coating. Testing was difficult to perform due to the high stiffness of the bitumens. Figure 21 shows a large crack which was easy to spot but a lot of small cracks also appeared and it was very difficult to see these small cracks during testing. Therefore, it is possible that the temperature at which cracks appear is actually higher than recorded. This supports findings by *Laukkanen* et al. (2013), where bitumens

tested proved to express ductile properties. Ductile materials develop so called crazes (micro-cracks) capable of load transfer prior to development of visible cracks. Results agree with penetration measurements as the softer binders had colder breaking temperatures.

In the specification (PANK 2000), the Fraass breaking point requirement for bitumen 70/100 is -10 °C and for bitumen 35/50 it is -5°C. Test results shown in Table 9 indicated vulnerability for thermal and fatigue cracking as bitumen was hard.

Figure 21. *Binder film cracking on Fraass breaking point measurement test: example of large crack easy to see and smaller cracks more difficult to detect by naked eye during testing.*

Frequency sweep tests were performed with a stress-controlled Reologica StressTech rheometer in the controlled-strain measurement mode. Measurements were done in the temperature range of 2-100 °C starting from the lowest temperature. Parallel plate geometries having diameters of 8 mm and 25 mm and measurement gaps of 2 mm and 1 mm were used in the temperature ranges of 2-40 °C and 50-100 °C, respectively. In all of the temperatures a frequency sweep from 0.01 Hz to 10 Hz was performed within the region of linear viscoelastic (LVE) response of the studied binders. These limits for LVE response were determined by strain sweep tests prior to the frequency sweep measurements.

Table 9. *Conventional and DSR measured bitumen properties. Excluding reference 70/100 binder, reading with yellow background is the stiffest and magenta is the softest result.*

Property	70/100	AB	C	E (slab)	G	J
Pen 1/10 mm at 25°C	66,5	9,8	13,7	17,0	16,5	17,7
Softening point, °C	47,5	73,6	66,9	-	64,8	65,0
Fraass breaking point, °C	-19	-2	-4	-	-4	-4
G* at 64°C (kPa)	1,11	11,14	69,71	23,37	21,79	19,59
δ at 64°C (deg)	86,84	75,18	65,87	73,28	72,74	74,05
G*/sin δ at 64°C (kPa)	1,11	11,52	76,38	24,40	22,81	20,37
G*sin δ = 5000 kPa (°C)	15	18	27	21	23	23

Again excluding the reference 70/100 binder, the Superpave PG-grading rutting parameter G*/sinδ at 10 rad/s given in Table 9 suggests that the softest binder was AB followed by E, G and J grouped quite closely together. Area C deviated from this group significantly having the

stiffest binder properties. The Superpave criteria for rutting requires that parameter G*/sinδ at 10 rad/s must exceed 1 kPa (AASHTO M320) to meet the specification. Binders extracted from Kehä II were thus vastly altered and hardened in comparison to the reference 70/100 binder. However, these results do not agree with the conventional test results, which needs to be studied further.

In Figure 22, a semi-logarithmic plot of phase angle δ against complex shear modulus G*, which is commonly known as Black diagram, is presented for the studied binders. From the plot it can be seen that extracted Kehä II binders exhibited relatively more elastic behavior compared to the reference 70/100 binder. However, no significant differences between the Black curves of aged Kehä II binders could be seen. Susceptibility to fatigue cracking can be predicted with the Superpave fatigue parameter G*sinδ, for which a critical temperature is defined to be the temperature at which G*sinδ = 5000 kPa (AASHTO M320). From Table 9 it can be seen that Kehä II extracted aged binders had considerably higher critical temperatures compared to 70/100 binder indicating vulnerability to fatigue cracking.

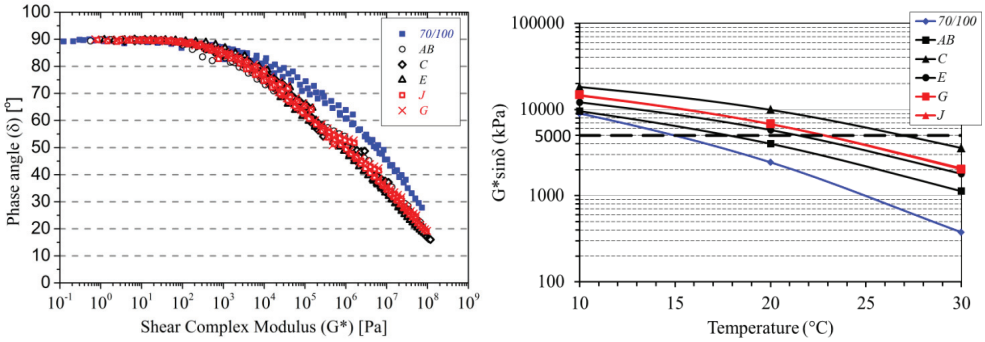

Figure 22: *Black curves (left) and Superpave fatigue cracking parameters G*sinδ (right). AB, C and E were Bad areas and J and G were Good areas.*

5.2 SARA Fractions

The generic fractions of the base bitumens were determined by thin-layer chromatographic (TLC) method with flame-ionization detector (IATROSCAN MK-6s). Bitumen samples, extracted and recovered as previously mentioned, were dissolved in chloroform and applied on chromarods. Saturates were eluted with n-heptane, aromatics with solution of toluene (80 %) and n-heptane (20 %) and resins with solution of dichloromethane (95 %) and methanol (5 %). Results are shown in Table 10.

Transformation of aromatic fraction into resin fraction stays in agreement with knowledge of bitumen aging (*Siddiqui* and *Ali* 1999, *Isacsson* and *Zeng* 1997). However, area G and C express similar levels of asphalthenes compared to the original bitumen. Similar observations were not found from literature dealing with aging of binders. Rehabilitated area G may contain a supplementary amount of softer binder and thus the reading of asphalthene may be on the lower scale (*Simonen* et al. 2013). The same cannot be stated for area C and this is currently under further investigation. Samples collected from area E resulted in extraordinary readings because there were no saturates or aromatics. Similar reports were not found in literature for laboratory aged binders, analyzed by TLC technique. Results indicate extreme degree of aging, though. Preliminary hypotheses based on the results above and the brown

color of asphalt mixture are that either bitumen was overheated during production or addition of some modifying agent caused instability and separation of bitumen into subcomponents.

Table 10. *SARA fractions for bitumens.*

Binder	**70/100**	**C**	**E**	**G**
Asphalthenes [%]	20	19,4	36,6	18,1
Resins [%]	27	51,1	57,6	41,7
Aromatic [%]	49	27,6	3	40,2
Saturates [%]	4	2	2	0

According to relation presented by *Isacsson* and *Zeng* (1997), the higher the combined abundance of asphalthenes and resins in bitumen, the higher the Fraass Breaking Point. Results presented in Table 10 suggest higher propensity of Kehä II extracted bitumens to cracking in temperatures close to zero or even above zero.

6 ADVANCED AGGREGATE AND FILLER PROPERTIES

Construction records and air temperature records from Finnish Meteorological Institute allowed estimating that air temperature, during paving work in fall 2002, was close to zero degrees. This cold temperature is possible origin for the poor compaction, in addition of possible deficiencies in raw materials and mixture composition, which will be studied further below. As discussed above, observations from binder extraction suggested that SMA 16 LTA mixture may contain fly ash instead of limestone filler specified by mix design. Hydrated lime ($Ca(OH)_2$) or calcium hydroxide, which is a high surface area powder commonly used in road construction, was a second possible additive used. This hypothesis was investigated as follows. First, the presence of limestone filler or lack of thereof was established via solubility testing and verified by TGA and XRD. Surface area measurements were conducted to exclude the overflow of low surface area aggregate fines and to confirm the addition of high surface area component. As CaO content could not be established according to EN459-2 due to presence of heavy metals, XRD was applied and it confirmed lack of calcium hydroxide in fines. Additional optical investigation of particle shape by SEM was conducted in order to confirm the presence of fly ash.

6.1 Test on Solubility in hydrochloric acid (HAST)

After gradation analysis of extracted aggregates, a fraction <0,063 mm from the samples collected from areas E, C and G were subjected to tests of hydrochloric acid (HCl_{aq}) solubility (PANK 2405), standard measurement required as supplemental information of any limestone fillers used in road construction in Finland. Method can be described as follows: 10 g of dry material is weighted in beakers and dried in oven at 110 ^{o}C, allowed to cool down for 1 hour in desiccators and weighted again, following addition of 50 ml of deionised water (DW) and 25 ml of concentrated HCl_{aq} (37 %). Such prepared samples are conditioned in boiling water bath for 30 min. Beaker residues are filtered on a medium filter paper (Whatman), previously dried in the oven at 110 ^{o}C, allowed to cool down in desiccator, and weighted. Filter with residue is dried in the oven at 110 ^{o}C for one hour after which samples are allowed to cool down to room temperature in desiccator and weighted again. **Mass loss**, recalculated into percent, provides a value of total solubility in HCl_{aq}. Reference tests for fly ash (FA_{HAST}=7,78

%) originated from biomass and crushed aggregate (AGG_{HAST}=4,91%) were conducted on fraction passing 0.063 mm sieve.

First, calculations were conducted on minus 0.063 mm fraction with an assumption that 78,1 % of limestone is passing 0.063 mm sieve, and 94,5 % - 0.125 mm sieve (QC report). Solubility i.e, HAST results for minus 0.063 fraction were found significantly lower than calculated for all the samples on the basis of Mix Design report (limestone $filler_{HAST}$=93.7 %) (see Appendix C).

According to construction specifications (PANK 2000), limestone filler needed to meet a criteria of HAST over 75 %, so-called CC75, incorporated in this report as minimal allowed value.

Second option was to investigate if filler with 75 % solubility was used This would indicate use of different type natural limestone filler, (see EN 13971) or that filler was diluted with non-soluble cheaper material, referred to further as an **additive**, so that it still met the criteria of CC75. Both calculated and measured results are gathered and presented in Table 9. Table shows that measured solubility values met the minimum criteria for 8 % filler content, but differed vastly from the actual mix design. Limestone filler constitution was investigated further as follows.

Table 11. *Hydrochloric acid solubility test results in comparison with calculated values*.

Calculations, HAST %				Measured HAST%		
Composition of minus 0,063 mm fraction	LS filler to aggr.	HAST% for LS[1]	Calc.	C	E	G
Min. spec requirement for MD[2]: 9% LS filler	71,0:29,0	CC75[3]	54,57	51,86	48,30	47,58
Max. MD requirement: 9% LS filler	71,0:29,0	CC93,7[4]	67,95			
8% LS filler	63,1:36,9	CC93,7[4]	60,93			
Min. spec req. if 8% LS filler	63,1:36,9	CC75[3]	49,14			

[1]) LS = limestone, [2]) MD = mix design, [3]) from PANK 2000, [4]) from QC measurement

6.2 Thermogravimetral Analysis (TGA) and Differential Thermal Analysis (DTA)

The thermogravimetric analyses were done in a thermobalance (Perkin Elmer Pyris 1 TGA) in air atmosphere (40 ml/min) by heating powders, passing through sieve size of 0.063 mm, up to 1000 °C with a relatively slow heating rate (5 °C/min).

Figure 21 represents mass losses recorded during annealing of the samples. On the basis of DTA graph of the fines, mass losses were divided into 3 regions (area 1, 2 and 3). Taking the TGA/DTA graph of aggregate annealing into account a 4th area was distinguished.

Mass loss in area 1 can be assigned to moisture and remaining dimethyl chloride present within fines after extraction. Area 2 cannot be clearly assigned to particular compound but is most likely due to decomposition of hydroxides (magnesium, calcium and iron compounds) (*Kulp* and *Trites* 1951). Judging from the shape of the peaks, mass loss is due to decomposition of more than one component (organic matter not excluded) and therefore providing convoluted spectrum.

The largest mass change was observed in the region of 556-779 °C (area 3), with minimum in DTA found at 755 °C. Mass loss equaled 21,641 % and was assigned to complete carbonate decomposition (calcite and dolomite) (*Cuthbert* and *Rowland* 1947). This mass loss corresponds to **47,45 - 49,98** % of carbonates in initial sample, and stays in agreement with results obtained through HAST (48,30 %, sample from area E).

Area 4, without clear DTA peak in the region but 1,26 % mass loss, is characteristic for organic compounds decomposition (humic acids, bitumen (*Jimenez-Mateos* et al. 1996), cellulose (*Khezami* et al. 2005), unburnt carbon, alumina-carbon). Organic matter in original aggregate, presented as reference, expresses mass loss within this region (0,11 %). It is not easy to distinguish between bitumen, cellulose or unburnt carbon from this measurement. However, it is worth noting that for sample, which would be consisting of filler substituted by 25 % of fly ash having a Loss of Ignition (LOI) of 2,8 % (min. reported) or 7 % (max. allowed, PANK 2008), the expected mass loss was 0,54 % or 1,37 %, respectively (*Fan* and *Brown* 2001).

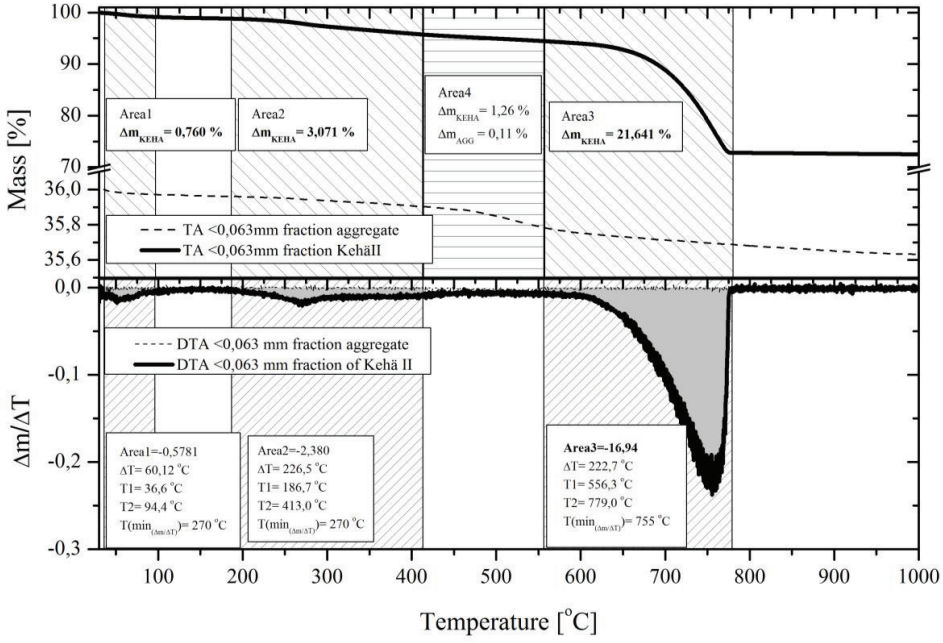

Figure 23. *TGA (a) and DTA (b) graph for sample E.*

6.3 X-Ray Diffraction (XRD)

Samples from area E were analyzed prior to and after TGA treatment with XRD. Phase identification of the samples was confirmed with a laboratory X-ray powder diffractometer (XRPD; PanAnalytical X'Pert PRO MPD, CuKα1 radiation) at room temperature in the 2θ range of 10 °C–100 °C.

XRD allows analyzing mineral matter on the basis of crystallographic structure, characteristic for every chemical compound. Amorphous phases such as molten glass raise the background during measurement indicating lower crystallic phase structure content.

Sample of Kehä II revealed high abundance of calcite and dolomite prior to TGA treatment. Analysis of sample after TGA revealed that a transition from calcite to calcium oxide and from dolomite to mixture of magnesium and calcium oxides occurred completely, according to the reactions given in (1) and (2):

$$CaCO_3 \rightarrow CaO + CO_2 \quad (1)$$
$$CaMg(CO_3)_2 \rightarrow CaO + MgO + 2\,CO_2 \quad (2)$$

Slight raise in background was recorded, yet not sufficient enough to conclude on the presence of fly ash.

Aggregate composition (Table 10) is consistent with known mineral composition of Koskenkylä aggregate (*Apilo* and *Eskola, 1998*). Stolzite can originate from not removed ink from the newspapers used in the production of cellulose fibers.

Table 12. *Mineral composition as defined by XRD***.**

Type of sample	Chemical formula	Name of the mineral	Abundance
Fines sample E prior to annealing	SiO_2 $CaCO_3$ $CaMg(CO_3)$ $(Na,Ca)Al(Si,Al)_3O_8$ $Pb(WO_4)$ unspecified	quartz calcite dolomite albite (plagioclase) stolzite amphibole	38.6% 18.8% 14.9% 25,7% 2% <1%
Aggregate prior to annealing	SiO_2 $Na(AlSi_3O_8)$ unspecified	quartz sodium tectoalumotrisilicate, i.e. plagioclase amphibole	-

6.4 Surface area (SA) analysis

Due to the fact that limestone, fly ash and aggregate dust (baghouse fines) are having different surface areas, this path was followed during investigation and surface area (N2-BET, Flowsorb II 2300, N2/He 30:70) was measured for fractions <0,063 mm. Table 13 represents obtained data. Unfortunately, data for the surface area of the additive investigated was not available in the documentation, yet QC Loss on Ignition (LOI) values for unspecified fly ash was found for September and October 2002 (See Appendix C). We plotted reported LOI values according to correlation derived from data provided in *Luo* et al. (2011) (Figure 24.).

As presented in Table 13, there exists a clear difference between contents of binder and fines fraction among collected samples. Dust/asphalt ratio for mix design was 9,9 %/6,1 % = 1,62 and for SA/binder 1,65/6,1= 0,27. As these values were higher for the samples, this indicates that mixture was dry and did not have enough binder. The SA/binder ratio correlated better with the performance than the actual dust/binder ratio.

Nevertheless, sample K containing more of fines of similar surface area as those investigated from areas A and B, was marked as good. The origin of good mechanical behavior of the sample was sought in its increased binder content in comparison with those found for all the bad samples (<6,0 %).

Table 13. *Measured and estimated surface areas. For LA, OA and HA see Figure 24.*

Property		Calc. SA [m^2/g]	Measured		
			K (good)	A, B (bad)	C (bad)
9% filler, 3:1 (LS:FA)	LA	2,5392	2,844 [m^2/g]	2,757 [m^2/g]	3,567 [m^2/g]
	OA	2,9688			
	HA	3,4551			
8% filler, 3:1 (LS:FA)	LA	2,4395			
	OA	2,8165			
	HA	3,2433			
9% filler, LS		1,6535[1)]			
Percent passing 0,063 mm sieves [%]			11,0	9,2	7,7
Binder content [%]			6,3	5,9	5,9
Dust/binder ratio			1,74	1,55	1,30
SA/binder ratio			0,45	0,47	0,61

[1)] Literature data (*Turunen* 1991): surface area measured by FlowSorp II 2300 for materials used in Finland: limestone filler (LS) - 1,61 m^2/g, baghouse fines - 1,76 m^2/g.

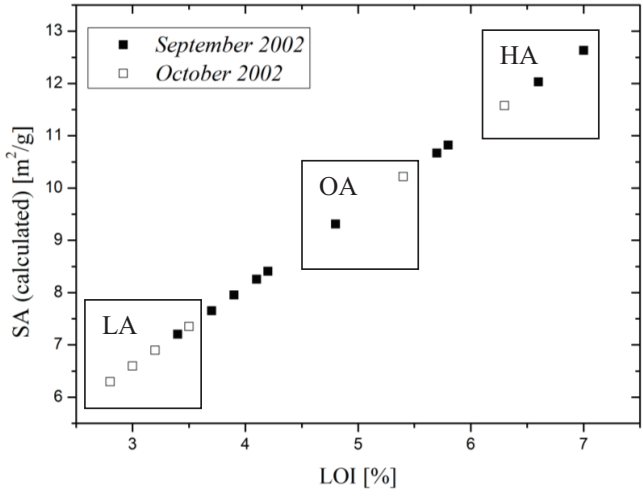

Figure 24. *Correlation between Loss on Ignition values and surface area. Squares mark the ranges of values used in Table 13. LA – low average, OA – overall average, HA – high average.*

6.5 Scanning Electron Microscopy (SEM)

With a prediction of fly ash presence in the filler, we set off to verify findings by investigating minus 0.063 mm fractions size distribution. As mentioned before, increased hydrophobicity of the samples and partial floatation prevented hydrometer analysis.

After extraction minus 0.063 mm fraction was additionally exhausted in vacuum (25 mbar) at room temperature, for a period of 30 minutes. Such prepared powder was mounted on the

microscope stub using copper-carbon tape. Image analysis was conducted with JEOL JSM-840 SEM.

Dominating shape within particle size of 100 µm was assigned to the coarse aggregate (Figure 25(A)). As magnification increased (Figure 25(B)), the dominant particle size became spherical, ovoid, amorphous or fractured spherical, which was assigned to the particles originating from fly ash.

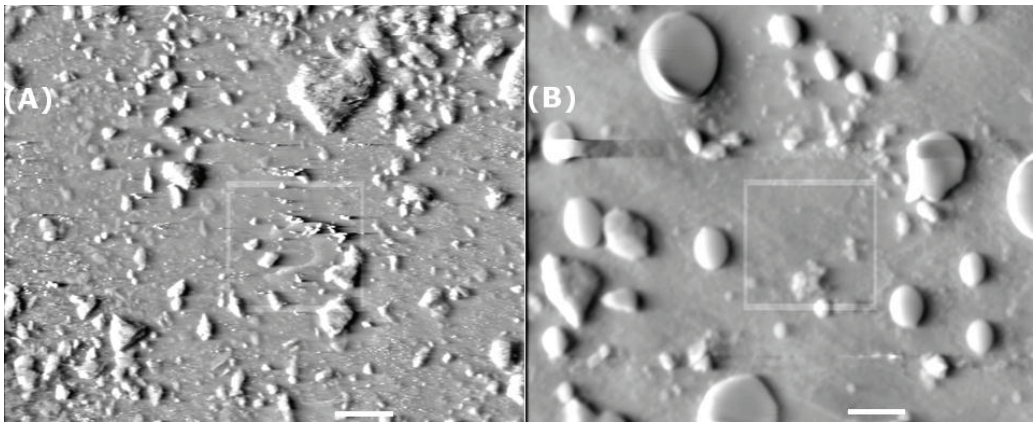

Figure 25. *Images of Kehä II fines, area E after extraction, fraction <0,063 mm. Legend bar indicates distance of (A) 100 µm and (B) 10 µm.*

7 DISCUSSION

7.1 Pavement distresses vs. mechanical properties

Research shows that the insufficient layer thickness combined with too cold laydown and compaction temperatures resulted in poor workability of mixture. This made it difficult to achieve the design compaction level, which produced areas with too high air voids content. In those areas, especially under bridges where the humidity is high, moisture was able to infiltrate into the pavement decreasing strength and durability of the asphalt.

Figure 26 summarizes measured stiffness and strength properties for Kehä II pavement layers. For all "bad" areas, the Indirect Tensile Strength was less than 1,5 MPa and Indirect Tensile Stiffness was less than 6500 MPa at 10 ºC. The strength properties were more affected than the stiffness of the mixture: strength in the bad areas was on average 44 % lower than in the good areas while stiffness reduction was 23 %. Figure 26 also shows that the Remix rehabilitation for layer (a) had restored mixture strength properties due to better compaction but did not seem to affect the stiffness properties.

For the newly laid fresh mixture (area O) stiffness was the lowest being 4572 MPa. For base mixture (ABK) stiffness was quite high being 18 787 MPa due to lower binder content and coarser gradation.

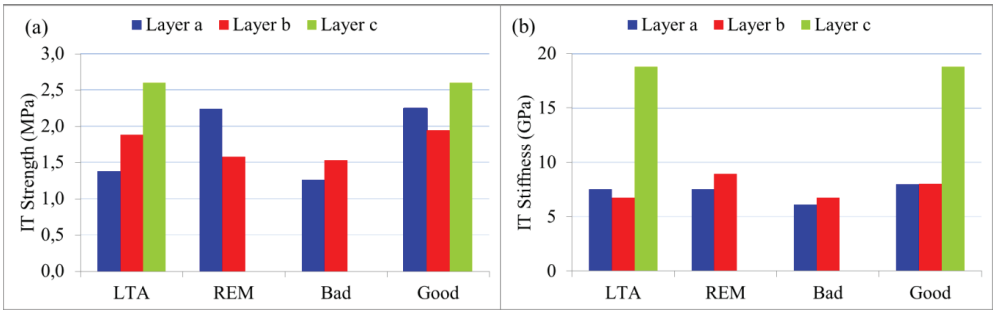

Figure 26. *Original 2002 (LTA) and rehabilitated REM sections vs. Bad and Good areas.*

Pellinen (2004) has proposed a conceptual formulation of the performance criteria for the asphalt mixtures, shown in Figure 27. These criteria were developed based on the analysis of three volumetric mix design specifications and this concept converts the diverse volumetric criteria to a fundamentally based mix design specification that uses mix stiffness and strength as performance parameters. The criteria is based on assumptions that if stiffness and strength are low, the potential for rutting (permanent deformation) due to heavy traffic increases but the potential for thermal cracking decreases; and if stiffness and strength are high, the potential for rutting decreases while the potential for thermal cracking increases. An increase in mixture strength decreases the potential for fatigue cracking, which increases the durability of the mix. An increase of mix stiffness either increases or decreases fatigue cracking depending on the pavement structure.

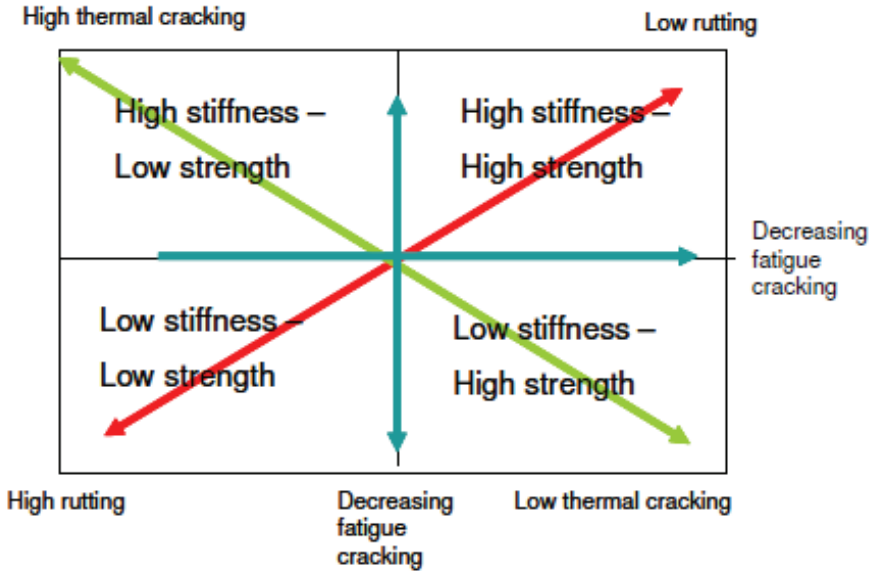

Figure 27. *Mixture performance criteria proposed by Pellinen (2004). Rutting here refers to permanent deformation caused by heavy truck traffic.*

Figure 28 plots stiffness and strength properties for Kehä II pavement layers. Missing values were estimated assuming linear correlation between stiffness and strength. Figure 28 shows that all "bad" areas are located in the "zone for low stiffness and strength".

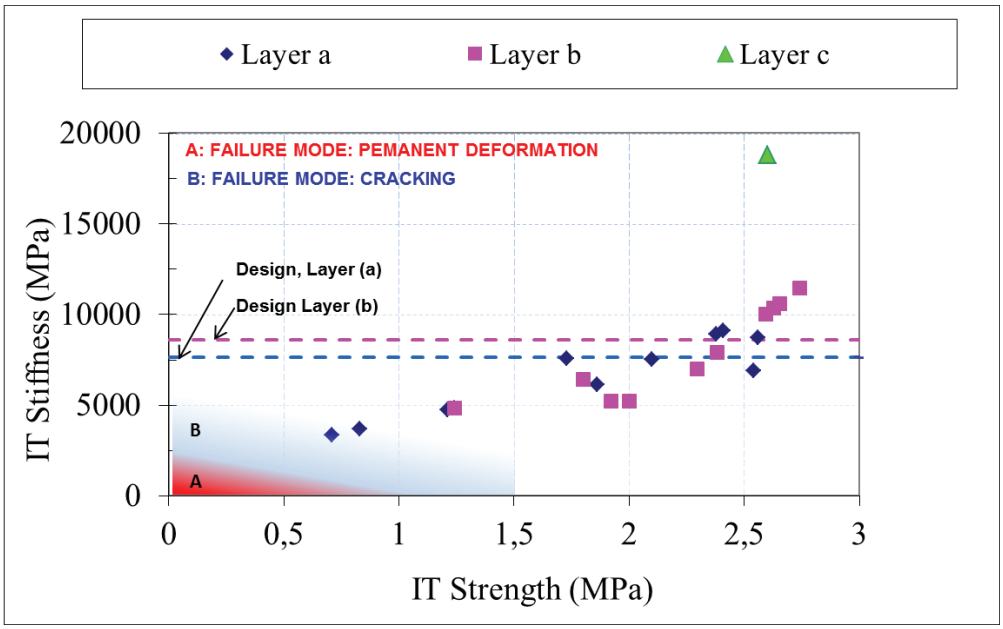

Figure 28. *Stiffness vs. strength properties can be used to estimate ductile and brittle mixture properties and to predict durability failure zone for asphalt mixtures.*

Kehä II pavement structure failed due to poor durability of asphalt mixtures which led to moisture damages, cracking, raveling and eventually pothole development. There was a small section of hot in-place remix paving applied only to rut depths on wheel paths, but rutting due to heavy traffic was not a problem for this road. The amount of rutting is determined by the pavement temperature and the amount of heavy traffic. Due to relatively low pavement temperatures in Finland, the major cause for rutting is usually pavement wear caused by studded tires. However, wear increases if mixture durability is compromised.

Based on Figure 28 it can be concluded that relative to performance temperature, the low stiffness and strength are governing the durability of the mixture, similarly to the propensity for rutting. The stiffness threshold value for cracking depends on the ability of binder to elongate due to fast loading at intermediate and cold temperatures. The absolute stiffness threshold value to resist permanent deformation depends on the ability of binder to resist shear flow due to slow loading at warm and hot temperatures. Both distresses accumulate with repetitive loading and are thus dependent on the amount of traffic. However, both distresses lead to rapid failure if load levels are high enough to cause large strains in the asphalt mixture.

It can be speculated that the failure zone for durability for typical SMA 16 mixtures used in Finland with the binder content of 6 % and 70/100 binder, is governed by Indirect tensile stiffness of less than 6 500 MPa and Indirect tensile strength of less than 1,5 MPa.

7.2 Proposed pavement durability distress mechanism

The lack of bonding between layers can be explained in two ways: either water that reaches the interface between layers was able to wash off binder due to horizontal water flow or there was not enough glue between layers in the first place. Whatever the reason, the consequence is that bound pavement layers did not form a monolithic layer structure. In this way the traffic load is able to cause horizontal displacements, which in turn are initiating micro-cracking (*Laukkanen* et al. 2013) and eventually these micro-cracks grow larger, the bond between aggregate and mastic is weakened and pavement starts exhibiting potholes and surface raveling. Figure 29 presents the proposed distress model mechanisms drawn from these findings.

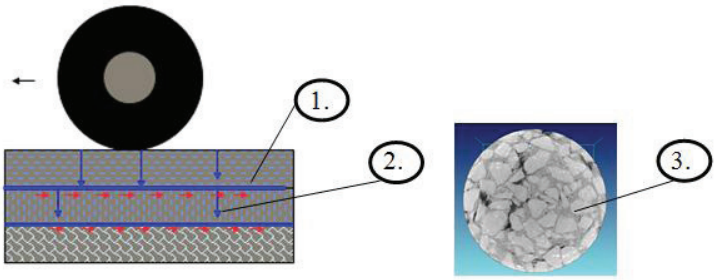

Figure 29. *Proposed pavement durability distress mechanism based on Kehä II findings.*

1. Bond separated surface layer is sliding back and forth in front of the wheel and shear stresses start to develop inside layers and within layer boundaries. This initiates and propagates pavement cracking intensified by the high air voids content in segregated and poorly compacted areas. Water from precipitation or melting snow can infiltrate into pavement from these cracks. Cracks keep building up when bitumen shrinks at winter time.

2. Hydrostatic pressure caused by pumping action by wheel loading is spreading inside the layers through crack cavities and this is causing upward lift of layers if they are not bonded properly.

3. As water is incompressible it creates high pressure inside small crack cavities and this combined with the pressure from the freeze-thaw action in the spring will weaken the bonding between aggregate and mastic, eventually causing raveling. The deterioration is intensified by vapor pressure build up in the mastic as the cold pavement surface is rapidly warming up during sunny spring days.

Furthermore, due to decreased stiffness resulting from separated asphalt layers, vertical traffic loading transmitted to the lower layers is more concentrated and causes larger deformations, which is decreasing fatigue life of asphalt layers and increasing damage. Therefore, the high air voids content and the lack of bonding between layers will cause pavement layers to further deteriorate with an increasing rate. The hot in-place remix rehabilitation work of certain areas helps to heal some of the cracked areas and due to re-compaction decease air voids in the wearing course. But this technique cannot restore the structural capacity of pavement that has been compromised. Therefore, pavement deterioration will expand underneath seemingly

good wearing course surface. We predict that soon potholes will appear again in the Kehä II surface layer.

7.3 Filler Substitution

Hydrochloric acid solubility tests indicated lower than designed content of limestone filler in fines fraction (<0,063 mm). Calculations indicated the use of limestone filler conforming to the filler specification of calcium carbonate content of over 75 %, CC75 (PANK 2000). Surface area measurements indicated the use of other filler component which was not of a natural source of origin. Exclusions by XRD and TGA, along measurement by SEM confirmed the presence of fly ash in the fines.

Use of filler other than the one denoted in mix design requires additional material characterization for fines (PANK 2000) or alternatively demonstration of suitability by performance-based mix design. Neither of the above was found from documentation.

On top of filler substitution, mix design was optimized for 9 % limestone filler content. However, results of this investigation indicate that 8 % or less of altered filler was used, and found binder content was on average 0,1 % lower than that of mix design. In addition, gradation analysis indicated problems with dust/binder ratio.

Furthermore, better parts of the road were found to have slightly higher binder content (0,2-0,4 %) than specified in the mix design or established for bad areas, respectively. As reported by *Zaniewski* and *Reyes* (2003), use of higher surface area filler in the same mix design increases rut resistance but decreases fatigue resistance. Observations on the rheological properties of binder stay in agreement with aforementioned and authors strongly believe, supported by literature, that insufficient amount of binder was used to meet the Rigden criteria of free binder (*Anderson* 1987, *Mogawer* and *Stuart* 1996). It is obvious that contractor failed to take this into account. As surface area of fines affects mastic hardening (e.g. ΔR&B) by reducing free binder content, the needed temperature for compaction is expected to rise for higher surface area filler (*Mogawer* and *Stuart* 1996). Problems in workability may have caused the higher air voids content (*Zoorob* et al.1997) due to handling issues, leading to more pronounced aging (*Whiteoak* 1990, Shell Bitumen Handbook) manifested in the SARA fractioning results. The observed brown color of mastic can be explained by the bitumen constituent separation hypothesis, when fractions responsible for lubrication (saturates and aromatics) are found missing (*Whiteoak* 1990, Shell Bitumen Handbook).

All of the above stays in agreement with findings of Kehä II and will be investigated further during the failure reconstruction stage of Phase II of this study.

8 CONCLUSIONS

Hydrochloric Acid Solubility Test (HAST), as a cheap and easily executable technique, proved to be an attractive preliminary stage test in forensic analysis of failed pavements. Data collected with it provided a hypothesis necessary in the troubleshooting to be verified by more expensive analysis techniques such as XRD, TGA, BET-surface area and SEM.

A reason for Kehä II premature pavement failure was found to originate from alteration of filler composition between the steps of mix design and construction. A foreign element added into the limestone filler was found to be fly ash. Lack of mix design verification led to increased binder/mastic viscosity, resulting in poor mixture workability and higher air voids content in laid pavement surface layer. This led to increased susceptibility to moisture damage, potholes and fatigue cracking.

Mechanical properties for the damaged pavement can be summarized as follows:

- For damaged areas the Indirect tensile strength was less than 1,5 MPa and the Indirect tensile stiffness was less than 6500 MPa measured at 10 ºC.
- The strength properties were more affected than the stiffness: strength in the "bad" area was on average 44 % lower while stiffness was 23 % lower than in the "good" area.
- Remix rehabilitation was able to restore strength properties due to re-compaction of the damaged layer but stiffness properties seemed to be unaffected.

The proposed asphalt **pavement durability distress mechanism** incorporating bitumen aging, damage caused by traffic loading and environmental aspects can be summarized as follows.

- In summertime asphalt "self-heals" its micro-cracks.
- In wintertime hard unmodified bitumen suffers micro-cracks in mastic due to lack of capacity to elongate and relax as bitumen shrinks
- In spring moisture infiltrates into the micro-cracks and washes bitumen from the aggregates with the help of the water pumping effect caused by traffic loading and vapor pressure created by pavement temperature increase. Pressure from freeze-thaw alterations and vapor pressure build up due to the increase in temperature weakens and deteriorates the cracked pavement.
- In the following summer aged and harder bitumen heals fewer cracks than in the year before. Water pumping and washing off bitumen keeps taking place.

Further research is warranted to investigate mastic and bitumen aging. It is envisioned that if other than limestone filler such as hydrated lime or fly ash will be used in Finnish asphalt mixtures, Rigden voids and increase in Ring and Ball softening point investigations should be conducted to verify the proper amount of binder in the mixture and the compatibility of raw materials.

Based on this investigation it can be hypothesized that to mitigate initiation of micro-cracking in pavements, it might be beneficial to use SBS modified binder with increased ability for elongation under thermal and traffic loading conditions. In addition, to improve bonding between aggregate and binder it might be cost effective to use some form of anti-stripping agent such as hydrated lime also in hot-mix asphalt. However, these hypotheses need to be verified with further research.

REFERENCES

American Association of State Highway and Transportation Officials (AASHTO), Standard Specification for Performance Graded Asphalt Binders M320, 2010

Anderson D. A., "Guidelines for use of dust in hot mix asphalt concrete mixtures", *Association of Asphalt Paving Technologists Proceedings Technical Sessions*, Volume 56, 1987, pp. 492-516, Reno, Nevada, USA

Apilo L., Eskola K., PAB-V-päällysteiden suunnittelu, Tielaitos, Tiehallinto, Helsinki, 1998, ISBN 951-726-396-1.

Apilo L., Eskola K., Uusiopäällystetutkimukset 1998, Tielaitoksen selvityksiä 7/1999, Helsinki 1999, ISBN 951-726-497-6

Cuthbert F. L., Rowland R. A., "Differential thermal analysis of some carbonate minerals", *American Mineralogists,* Volume 32*,* Issue 3-4, 1947, pp. 111-116

Fan M., Brown R. C., "Comparison of the Loss-on-Ignition and Thermogravimetric Analysis Techniques in Measuring Unburned Carbon in Coal Fly Ash", *Energy & Fuels*, Volume 15, Issue 6, 2001, pp. 1414-1417

Farcas F., "Evaluation of Asphalt Field Cores with Simple Performance Tester and X-ray Computed Tomography", Licentiate Thesis, Swedish Royal Institute of Technology, Stockholm, 2012

Finnish Asphalt Specifications 2000, Finnish Pavement Technology Advisory Council (PANK), Edita Ltd, Helsinki, 2000, ISBN 951-97197-6-8

Finnish Asphalt Specifications 2008. Finnish Pavement Technology Advisory Council, (PANK), Edita Ltd, Helsinki, 2007, ISBN 978-952-99985-0-0

Isacsson U., Zeng H., "Relationships between bitumen chemistry and low temperature behaviour of asphalt", *Construction and Building Materials,* Volume 11, Issue 2, 1997, pp. 83-91

Jiménez-Mateos J. M., Quintero L. C., Rial C., "Characterization of petroleum bitumens and their fractions by thermogravimetric analysis and differential scanning calorimetry", *Fuel*, Volume 75, Issue 15, 1996, pp. 1691-1700

Khezami L., Chetouani A., Taouk B., Capart R., "Production and characterisation of activated carbon from wood components in powder: Cellulose, lignin, xylan", *Powder Technology,* Volume 157, Issue 1, 2005, pp. 48-56

Kulp L., Trites A.F., "Differential thermal analysis of natural hydrous ferric oxides", *American Minearologist*, Volume 36, 1951, pp. 23-44

Laukkanen O. V., Pellinen T., Makowska M., "Exploring the Observed Rheological Behaviour of In-Situ Aged and Fresh Bitumen Employing the Colloidal Model Proposed for Bitumen", In: Multi-Scale Modeling and Characterization of Infrastructure Materials, Springer Netherlands, pp. 185-197, ISBN 978-94-007-6877-2

Luo Y., Giammar D. E., Huhmann B. L., Catalano J. G., "Speciation of Selenium, Arsenic, and Zinc in Class C Fly Ash", *Energy & Fuels*, Volume 25, Issue 7, 2011, pp. 2980–2987

Mogawer W. S., Stuart K. D., "Effects of fillers on properties of stone matrix asphalt mixtures", *Transportation Research Record: Journal of the Transportation Research Board*, Volume 1530, 1996, pp. 86-94

Pellinen T. K., "Conceptual Performance Criteria for Asphalt Mixtures", *Journal of the Association of Asphalt Paving Technologists*, Volume 73, 2004, pp. 337-366

Pihlajamäki J., Sikiö J., HSV-NORDIC Research Report No 2, Finnra Reports 29/2001, Finnish Road Administration, Helsinki, 2001, ISBN 951-726-764-9

Siddiqui M. N., Ali M. F., "Studies on the aging behavior of the Arabian asphalts", *Fuel*, Volume 78, Issue 9, 1999, pp. 1005-1015

Simonen M., Blomberg T., Pellinen T., Makowska M., Valtonen J., "Curing and aging of biofluxed bitumen: a physicochemical approach", *Road Materials and Pavement Design*, Volume 14, Issue 1, pp. 159-177

Whiteoak D., The shell bitumen handbook, Shell Bitumen UK, 1990, ISBN 0-9516625-0-3

Turunen R., Asfalttipäällysteiden täytejauheet, VTT, January 1991

Zaniewski P., Reyes C., "Evaluation of the effect of fines on asphalt concrete", Asphalt Technology Program, Department of Civil and Environmental Engineering, Morgantown, West Virginia, June 2003

Zoorob, S.E., Cabrera, J.G., Design and construction of a road pavement using fly-ash in hot rolled asphalt, Studies in Environmental Science, *Waste Materials in Construction — Putting Theory into Practice*, Volume 71, 1997, Pages 149–165

.

Appendix A: Core locations and test results

The following pages present core locations, test results and photograph of cores. Layers follow the nomenclature shown in figure below. In area L there is leveling course mixture placed between layers (b) and (c), which is designated as layer (d). In area L and O there are leveling course mixture placed between layers (a) and (b), which is designated as layer (d).

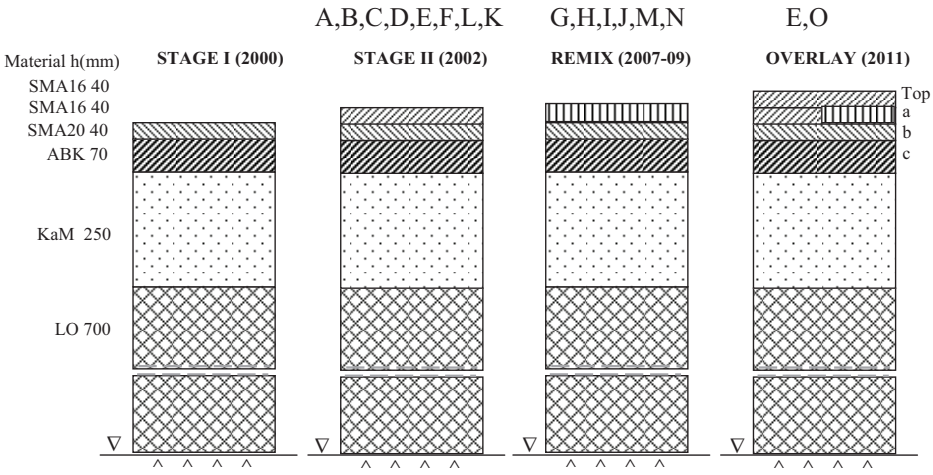

Table: Estimated and measured mixture maximum density values for different mixtures and mixture combinations. Due to large aggregates in layer c, the maximum density values ranged from 2,437 (binder content 5,6 %) to 2,470 (binder content 4,8 %). However, based on quite high pavement density values, an estimated value of 2,490 was used for calculations to avoid negative air void values. Also for area M and N, an estimated value of 2,437 was used.

	Estimated			Measured
Layer	binder content (%)	aggr. blend density (Mg/m^3)	max. density (Mg/m^3)	max. density (Mg/m^3)
Top	-	-	-	2,569
a	6,0	2,682	2,443	2,443
b	6,0	2,682	2,443	2,443
c	4,8	2,682	2,490	2,437-2,470

- White background color indicates that core was sawed and layers separated and tested.
- Magenta background color and text Not Tested (NT) indicates that sample maximum density was not measured but estimated based on measurements on that location.
- Blue background color and txt Not Separated and Tested (NS&T) indicates that for that particular core sample pavement density was measured without separating layers. The air void content of entire core was then calculated using estimated mixture density values given in parenthesis. Table below gives values that were used for air void content estimations.
- Yellow background color with text NS&T indicates that core was sent to KTH for X-Ray Scanning.

Location: Kehä II: Southbound direction	Lane: 22: **SMA 16 LTA 2002**	Area: A

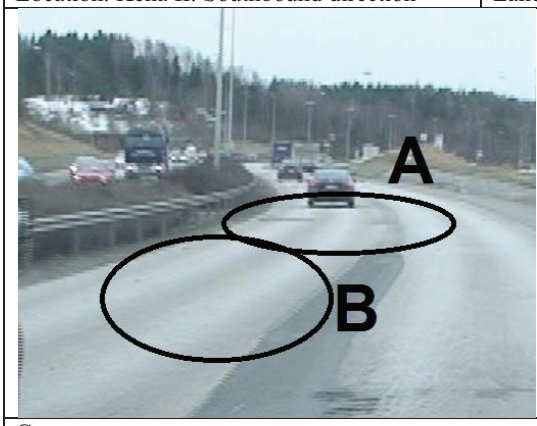

Coordinates: 60 11' 35'' N 24 44' 39'' E

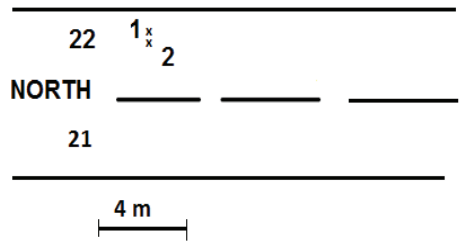

Sample distance 20 cm

Comments:
This was a badly deteriorated area, which has been patched several times. The layer (a) from the sample A 22 1 was not attached to the layer (b). The layer (c) could not be obtained. The layers (a) and (b) from the A 22 2 were glued together but the layer (c) could not be obtained.

SAMPLES	**A 22 1 a**	**A 22 2 a b (NS&T)**
Thickness (mm)	a = 32,54	a=27,66 ; b=76,39
Air voids content (%)	a=6,8 (2,452)	ab=4,6 (2,440)
Bulk density ρ_b (Mg/m^3)	a=2,286	ab=2,327
COMBINED SAMPLE	**A 22 1 a + B 22 1 a + 22 B 3 a**	
Max. density, ρ_m (Mg/m^3)	2,452	
Coarse aggr. density ρ Mg/m^3	2,699 (fraction 11,2-16 mm)	
Binder content (%)	5,9	
Penetration, Soft. Point (°C), Fraass (°C)	Pen 9,8; SP 73,6°C; Fraass -2°C	
Other tests	surface area analysis, DSR	
X-Ray Scanning	NO	NO

Size (mm)	**%-passing 1a +1a +3a**
22.4	100
16	97,8
11.2	62,6
8	33,3
4	24,8
2	22,4
1	19,4
0.5	17,1
0.25	14,8
0.063	9,2

Location: Kehä II: Southbound direction	Lane: 22: **SMA 16 LTA 2002**	Area: B

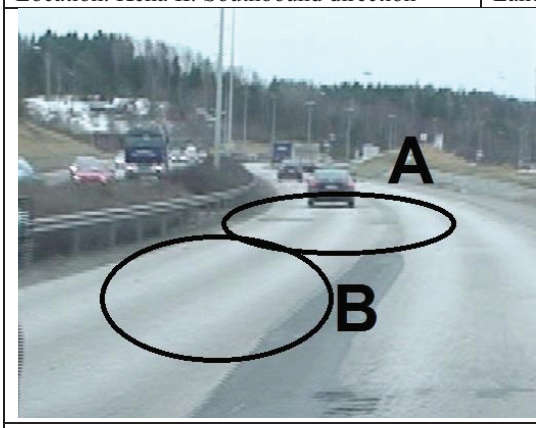

Coordinates: 60 11´35´´ N 24 44´38´´E

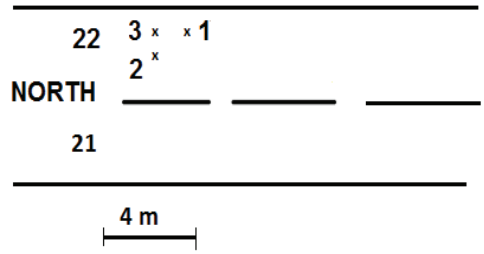

Distance between samples 40 cm

Comments:
This was seemingly a good area. The samples were drilled at some distance from the patches.
The upper layer was not attached to the bottom layer. The sample B 22 2 was damaged during coring

SAMPLES	**B 22 1 a**	**B 22 3 a**	**B 22 2 a (NT)**	**B 22 3 bc (NS&T)**
Thickness (mm)	a= 34,89	a=35,62	a=23,46	b=61,65 c=50,14
Air voids content (%)	a=7,6 (2,452)	a=8,2 (2,452)	a=5,7 (2,452)	bc=2,8 (2,478)
Bulk ρ_b (Mg/m^3)	a=2,266	a=2,250	a=2,312	bc=2,408
COMBINED	**A 22 1 a + B 22 1 a + 22 B 3 a**			
Max. ρ_m (Mg/m^3)	2,452			
Coarse aggr. ρ (Mg/m^3)	2,699 (fraction 11,2/16 mm)			
Binder content (%)	5,9			
Penetration, Soft. Point (°C), Fraass (°C)	Pen 9,8; SP 73,6 °C; Fraass -2 °C			
Other tests	surface area analysis, DSR			
X-Ray Scanning	NO		NO	NO

Size (mm)	**%-passing 1a +1a +3a**
22.4	100
16	97,8
11.2	62,6
8	33,3
4	24,8
2	22,4
1	19,4
0.5	17,1
0.25	14,8
0.063	9,2

Location: Kehä II: Southbound direction	Lane: 22: **SMA 16 LTA 2002**	Area: C

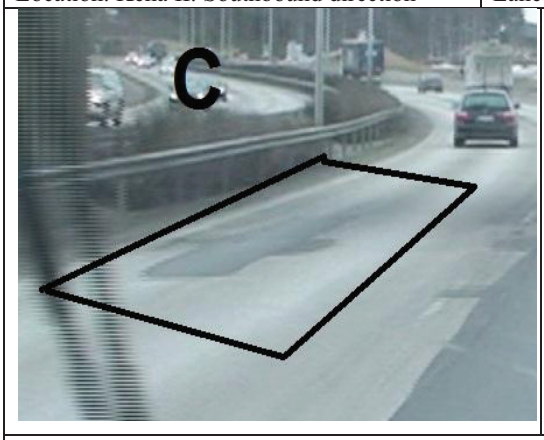

Coordinates: 60 11´ 37´´ N 24 44 38 E

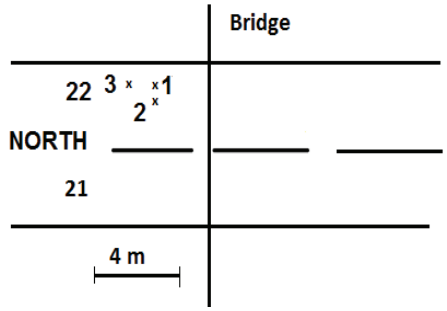

Distance between samples 20 cm

Comments:
There was a bad area under the bridge with several patches. It was not possible to take samples close of patched areas because mixture disintegrated during coring. The upper layer was not attached to the bottom layer. The samples were difficult to get out of the drill. The sample C 22 3 (a) split into two during coring.

SAMPLES	**C 22 1 a**	**C 22 2 a**	**C 22 3 a (NT)**
Thickness (mm)	a= 40,60	a=29,42	a=30,7
Air voids (%)	a=7,6 (2,454)	a=6,3 (2,454)	a=5,6 (2,454)
Bulk ρ_b (Mg/m^3)	a=2,267	a=2,300	a=2,317
COMBINED	**C 22 1 a + C 22 2 a**		
Max. ρ_m Mg/m^3	2,454		
Coarse and fine aggr. density ρ (Mg/m^3)	2,74 (fraction 11,2/16) 2,69 (fraction 0,063/0,125)		
Binder content (%)	5,9		
Penetration, Soft. Point (°C), Fraass (°C)	Pen 13,7; SP 66,9 °C; Fraass -4 °C		
Other tests	SARA, Surface area, DSR, HAST		
X-Ray Scanning	NO		NO

Size (mm)	**%-passing 1 a + 2 a**
22.4	100
16	96,2
11.2	63,8
8	32,7
4	23,9
2	21,9
1	18,8
0.5	16,5
0.25	14,0
0.063	7,7

Location: Kehä II: Southbound direction	Lane: 22: **SMA 16 LTA 2002**	Area: D

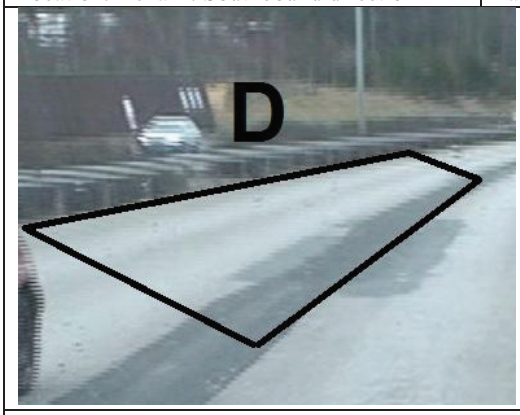

Coordinates: 60 11´ 22´´ N 24 44 51 E

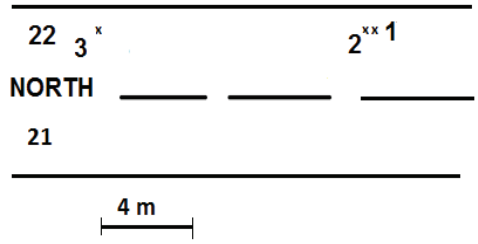

Distance between 3&2 12m, between 1&2 20cm

Comments:
This was visibly a good area.
The samples seem to be in good condition and the layers were well glued. However, the layer (a) of the sample D 22 3 was destroyed during release from the drill.

SAMPLES	**D 22 1 a b**	**D 22 2 a b**	**D 22 3 b c**
Thickness (mm)	a= 46 b=77,33	a=43,24 b=78,83	b=55,89 c=61,28
Air voids (%)	a= 4,7 (2,445) b= 2,0 (2,443)	a= 6,7 (2,445) b= 1,8 (2,443)	b= 5,0 (2,443) c= 1,4 (2,490)
Bulk ρ_b (Mg/m^3)	a=2,329 b=2,395	a=2,280 b=2,399	b=2,322 c=2,454
IT Strength (MPa)	a=1,83	a=1,63	b= not possible
IT Stiffness (MPa)	a=9013	a=6120	b=10008
COMBINED	**D 22 1 a + D 22 2 a**		
Max. ρ_m (Mg/m^3)	a=2,445		
X-Ray Scanning	NO	NO	NO

Location: Kehä II: Southbound direction	Lane: 22: **SMA 16 LTA 2002**	Area: E

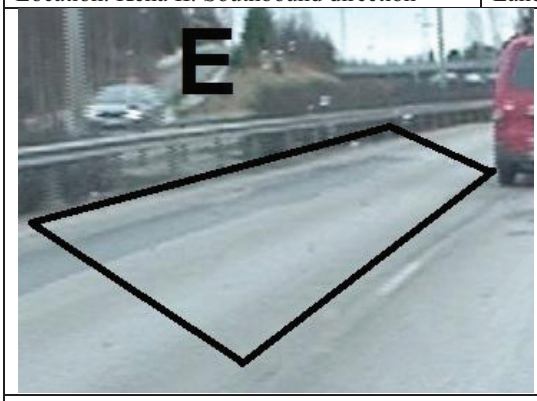

Coordinates: 60 11´22´´ N 24 44´56´´E

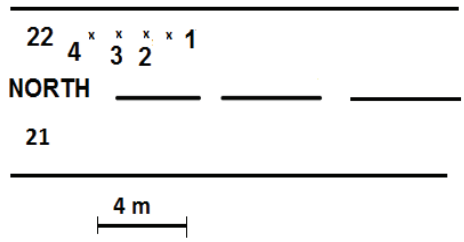

Distance between samples 1m

Comments:
This was a bad area that has been patched several times.
It was only possible to recover the first layer.

SAMPLES	**E 22 1 a**	**E 22 4 a**	**E 22 2 a (NT)**	**E 22 3 a (NT)**
Thickness (mm)	a= 34,49	a= 43,73	a= 40,68	a= 38,03
Air voids (%)	a=5,2 (2,437)	a=7,3 (2,437)	a=5,9 (2,437)	a=6,9 (2,437)
Bulk ρ_b (Mg/m^3)	a=2,310	a=2,259	a=2,292	a=2,270
IT Strength (MPa)	a=1,45	a=1,02		
COMBINED	**E 22 1 a + E 22 4 a**			
Max. density ρ_m (Mg/m^3)	2,437			
X-Ray Scanning	NO		NO	NO

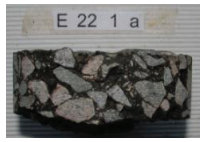

Location: Kehä II: Southbound direction	Lane: 22: **SMA 16 LTA 2011**	Area: E

Coordinates: 60 11´22´´ N 24 44´56´´E

Comments:
A new sample was taken from the area E on the 2nd of January 2012 after the road was overlaid again in 2011. Therefore this sample has 4 layers (Top layer = TL, a, b, c)

SAMPLES	**E SLAB**	**E 22 5 a (slab)**	**E 22 6 a (slab)**	**E 22 7 a (slab)**
Thickness (mm)	TL=41,61 a=34,55 b=66,18 c=45,26			
Max. density ρ_m (Mg/m^3)	TL=2,497			
Binder content (%)	a=6,2	a=6,2	a=6,1	a=5,7
Penetration		a=28	a=17	a=17
Other tests			SARA, DSR, HAST, TGA, XRD, SEM	SARA, DSR
X-Ray Scanning	NO	NO	NO	NO

Size (mm)	**%-passing**	
	TL	**5 a**
22.4	100	100
16	86,1	95,2
11.2	52,9	56,4
8	39,8	35,2
4	25,5	26,9
2	20,4	24,5
1	17,7	21,3
0.5	15,6	18,6
0.25	13,7	16,2
0.063	9,6	11,0

Location: Kehä II: Southbound direction	Lane: 22: **SMA 16 LTA 2002**	Area: F

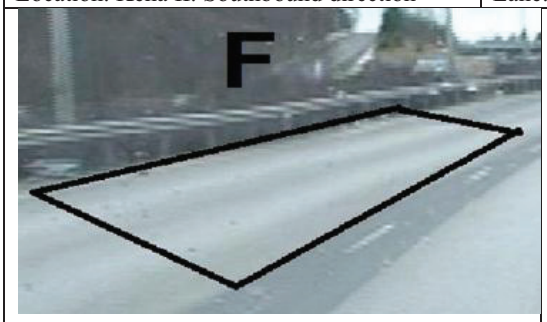

Coordinates: 60 11´13´´ N 24 44´56´´E

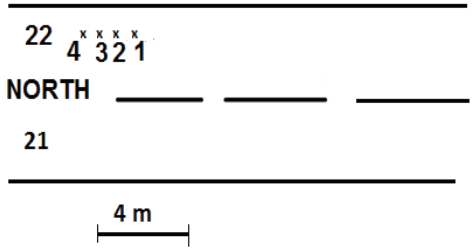

Distance between samples 40cm

Comments:
This was visibly a good area.
Only the first layer could be recovered, except for the last sample, which included also part of the second layer.

SAMPLES	**F 22 1 a**	**F 22 2 a**	**F 22 3 a (NT)**	**F 22 4 ab**
Thickness (mm)	a= 36,37	a= 33,59	a= 32,47	a=33,98 b=67,75
Air voids content %	a=5,7 (2,450)	a=5,9 (2,450)	a=6,3(2,450)	a= 5,6 (2,450) b=7,2 (2,443)
Bulk density ρ_b (Mg/m^3)	a=2,311	a=2,305	a=2,295	a=2,314 b=2,267
IT Strength (MPa)	a=1,06	a=1,37		a=1,19
IT Stiffness (MPa)	a=not possible	a=not possible		a= not possible b=7889
COMBINED	**F 22 1 a + F 22 2 a**			
Max. density ρ_m (Mg/m^3)	2,450			
X-Ray Scanning	NO	NO	NO	NO
				

Location: Kehä II: Southbound direction	Lane: 21: **SMA 16 REM 2007**	Area: G

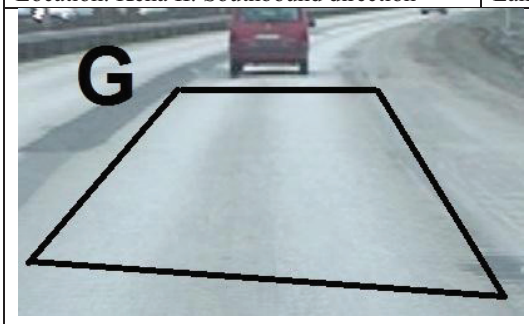

Coordinates: 60 11' 18'' N 24 45' 04'' E

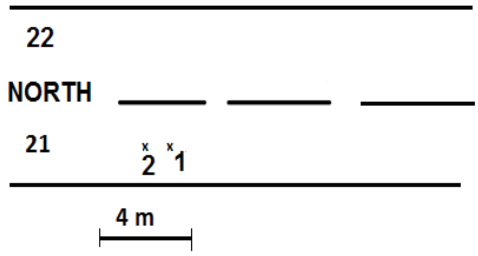

Distance between samples 1 m

Comments:
This was visibly a good area. All three layers for both samples were attached.

SAMPLES	**G 21 1 a b c**	**G 21 2 a b c**
Thickness (mm)	a=38,1 b=61,18 c=48,43	a=34,33 b=56,27 c= 53,96
Air voids content %	a= 2,6 (2,430) b= 4,6 (2,443) c= 1,5 (2,490)	a= 2,9 (2,430) b= 3,6 (2,443) c= 1,8 (2,490)
Bulk density ρ_b (Mg/m^3)	a=2,368 b=2,330 c=2,452	a=2,359 b=2,356 c=2,446
IT Strength (MPa)	a=2,56	a=2,51
IT Stiffness (MPa)	a=7033	a=6729 b=10341
COMBINED SAMPLE	**G 21 1 a + G 21 2 a**	
Max. density ρ_m (Mg/m^3)	2,430	
Binder content (%)	6,1	
Penetration, Soft. Point (°C), Fraass (°C)	Pen 16,5; SP 64,8 °C; Fraass -4 °C	
Other tests	DSR	
X-Ray Scanning	NO	NO

Size (mm)	%'passing	
	G1.2a	
22.4	100,0	
16	98,7	
11.2	70,8	
8	42,9	
4	27,6	
2	24,0	
1	19,2	
0.5	15,8	
0.25	13,2	
0.063	7,4	

Location: Kehä II: Southbound direction	Lane: 21: **SMA 16 REM 2007**	Area: H

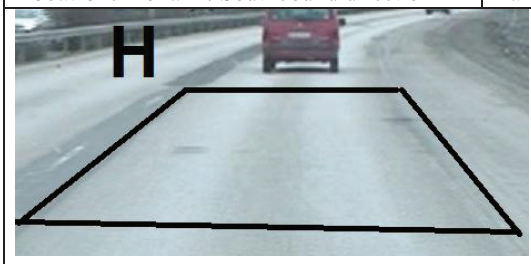

Coordinates: 9 meters north from G

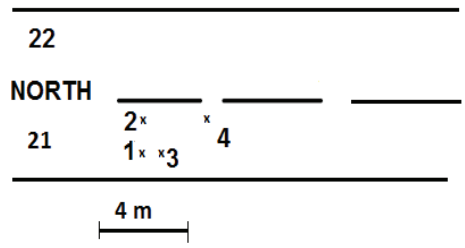

Distance between 1&2 1,5m, 1&3 1m and 2&4 3m

Comments:
This was a bad area that has been patched.
The first sample came out from the drill in three parts. The first layer was not attached to the layer (b).

SAMPLES	**H 21 1 a b c**	**H 21 3 a b c**	**H 21 2 a b c (NT)**	**H 21 4 a b c (NS)**
Thickness (mm)	a= 37,81 b=65,78 c=63,78	a=31,27 b=54,22 c=64,62	a= 43,52 b=55,77 c=46,00	a=39,22 b=53,92 c=63,83
Air voids content %	a= 6,1 (2,436) b=6,6 (2,443) c=2,1 (2,490)	a=6,3 (2,436) b=5,6 (2,443) c=2,0 (2,490)	abc=4,6 (2,460)	abc=4,1 (2,466)
Bulk density ρ_b (Mg/m^3)	a=2,288 b=2,281 c=2,437	a=2,283 b=2,306 c=2,440	adc=2,371	abc=2,366
IT Strength (MPa)	a=not possible	a=0,83		
IT Stiffness (MPa)	b=not possible	b=7015		
COMBINED	**H 21 1 a + H 21 3 a**			
Max. density ρ_m (Mg/m^3)	a=2,436			
X-Ray Scanning	NO	NO	NO	YES
				

Location: Kehä II: Southbound direction	Lane: 21: **SMA 16 REM 2007**	Area: I

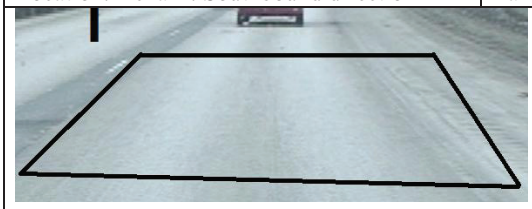

Coordinates: 60 11' 19'' N 24 45' 04'' E

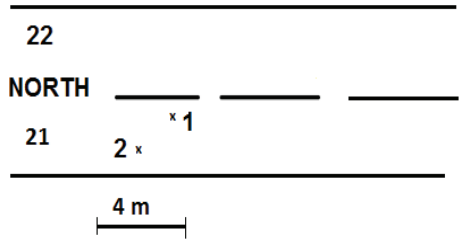

Distance between 1&2 2,25 m

Comments:
This was visibly a good area. All the three layers of both samples were bonded together.

SAMPLES	**I 21 1 a b c**	**I 21 2 a b c (NS&T)**
Thickness (mm)	a=46,02 b=60,9 c=56,3	a=50,1 b=61,39 c= 52,3
Air voids content %	a=3,1 (2,430) b= 4,9 (2,443) c= 0,0 (2,490)	abc=3,3 (2,459)
Bulk density ρ_b (Mg/m^3)	a=2,354 b=2,324 c=2,489	abc=2,378
IT Strength (MPa)	a=2,56	
IT Stiffness (MPa)	a=8708 b=10596	
Max. density ρ_m (Mg/m^3)	a=2,430 c=2,470 (too low compared to ρ_m)	
Binder content (%)	a=5,9 c=4,8	
Penetration, Soft. Point (°C), Fraass (°C)	Pen 17,7 SP 65 °C	
X-Ray Scanning	NO	YES

Size (mm)	**%-passing I1c**
31.5	100
22.4	100
11.2	58
8	46
4	30
0.5	13
0.063	2,1
	Too fine to meet the spec.

Location: Kehä II: Southbound direction	Lane: 21: **SMA 16 REM 2007**	Area: J

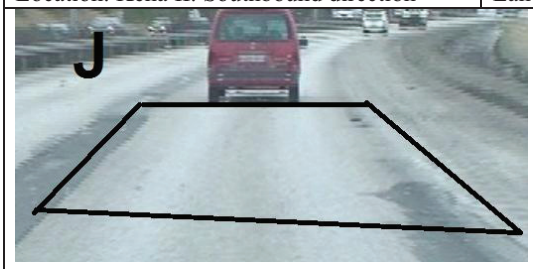

Coordinates: 10 meter north from I

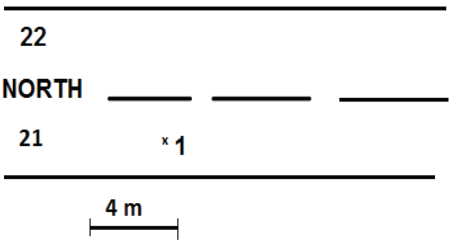

Comments:
This was a bad area with full of patches. The coring was done far from the patches.
The bond between layers (a) and (b) was weak.

SAMPLES	**J 21 1 a b c**
Thickness (mm)	a=45,11 b=56,38 c=51,78
Air voids content %	a=3,0 (2,441) b= 3,8 (2,443) c= 1,0 (2,490)
Bulk density ρ_b (Mg/m^3)	a=2,368 b=2,351 c=2,464
Max. density ρ_m (Mg/m^3)	a=2,441
Binder content (%)	a= 5,9
IT Strength (MPa)	a=2,41
IT Stiffness (MPa)	a=9115 b=11464
Penetration, Soft. Point (°C), Fraass (°C)	Pen a=17,7; SP a= 65,0 °C; Fraass -4 °C;
Other testing	DSR
X-Ray Scanning	NO

Size (mm)	**%-passing J1a**
22.4	100,0
16	99,0
11.2	66,0
8	39,0
4	27,5
2	25,0
1	21,1
0.	18,1
0.25	15,7
0.063	10,4

Location: Kehä II: Northbound direction	Lane: 12: **SMA 16 LTA 2002**	Area: K

Coordinates: 60 10' 40'' N 24 45' 29'' E

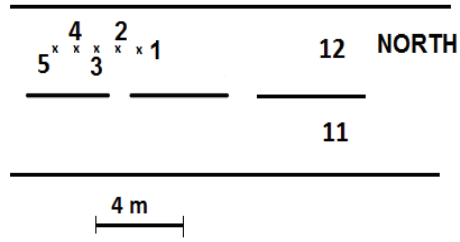

Distance between samples 90 cm
and distance to the shoulder 1,8 m

Comments: This was a good area. All the three layers were bonded together.

SAMPLES	**K 12 1 a b c**	**K 12 3 a b c**	**K 12 2 a b c**	**K 12 4 a b c (NS&T)**	**K 12 5 a b c (NS&T)**
Thickness (mm)	a=40,25 b=47,10 c=47,77	a=43,78 b=44,20 c=57,47	a=41,07 b=48,81 c=59,16	a=41,44 b=45,66 c=62,47	a=42,35 b=45,55 c=71,02
Air voids content %	a=4,2 (2,449) b=1,3 (2,487) c= 1,8 (2,437)	abc=2,2 (2,449)	a=4,3 (2,449) b=1,2(2,487) c=2,6 (2,437)	abc=4,4 (2,484)	abc=3,5 (2,485)
Bulk density ρ_b (Mg/m^3)	a=2,346 b=2,454 c=2,392	abc= 2,405	a=2,343 b=2,458 c=2,373	abc=2,374	abc=2,399
Binder content (%) , fines and finer content (%)		c=5,06	a=6,3, (fines = 11%, fibers = 0,136%)		
IT Strength (MPa)	a=2,26		a=1,93 b=2,00 c=2,60		
IT Stiffness (MPa)	a=9032 b=6084		a=5978 b=4344 c=18747		
COMBINED	**K 12 1 a + K 12 3 a**				
Max. density ρ_m (Mg/m^3)	a=2,449	c =2,437	a=2,434 b=2,487		
Other testing			surface area		
X-ray Scanning	NO	NO	NO	NO	NO

Size mm	**%-p K3c**
31.5	100
22.4	85
11.2	70
8	56
4	39
0.5	16
0.063	1,5

Location: Kehä II: Northbound direction	Lane: 12: **SMA 16 LTA 2002**	Area: L

Coordinates: 60 10’ 55’’ N 24 45’ 02’’ E

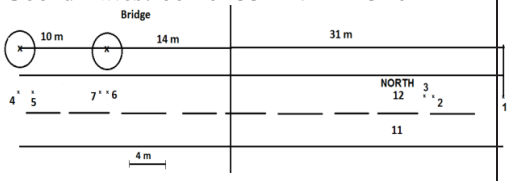

Distance 1&2 8 m; 2&3 1m; 4&5 1,5m; 6&7 1m

Comments:
This was a bad area that has been patched several times.
The first sample released from the drill in three parts. Layer (a) was not attached to the (b) layer. There was leveling course mixture (d) place between layers (b) and (c).

SAMPLES	**L 12 1 a b c**	**L 12 2 a b c d**	**L 12 3 a b c (NS&T)**	**L 12 4 a b c (NT)**
Thickness (mm)	a= 35,6 b=65,67	a= 32,98 b=45,63 d=27,38 c=73,49	a=35,07 b=44,98 d=22,79	a=37,67 b=53,12 c=25,80
Air voids content (%)	a= 8,9 (2,451) b=6,1 (2,424)	a=8,2 (2,451) b=6,4 (2,424) c=4,6 (2,490)	abd=4,5 (2,345)	a=9,7 (2,451) b=5,5 (2,424)
Bulk density ρ_b (Mg/m^3)	a=2,238 b=2,276 d=2,214	a=2,251 b=2,268 d=2,247 c=2,375	abd=2,240	a=2,214 b=2,290 d=2,278
IT Strength (MPa)	a= not possible	a=0,934 b=2,14		
IT Stiffness (MPa)	b=5831	b=6878		
COMBINED SAMPLE		**L12 2 a+L12 7 a L12 2 b+L12 5 b**		
Max. density ρ_m (Mg/m^3)		a=2,451 b=2,424		
X-Ray Scanning	NO	NO	NO	NO
			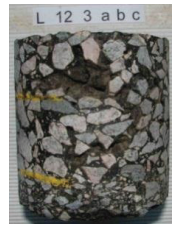	

SAMPLES	**L 12 5 a b d**	**L 12 6 b d c**	**L 12 7 a b d c**
Thickness (mm)	a=36,04 b=45,99 d=23,38	b=50,7 d=21,21 c=64,77	a=32,88 b=52,01 d=21,4 c=80,1
Air voids content Estimated (2,457)	a=7,3(2,451) b=6,4 (2,424)	b=6,7 (2,424) c=2,4 (2,490)	a=5,6 (2,451) d=0,9 (2,424) c= 2,2 (2,490)
Bulk density ρ_m (Mg/m^3)	a=2,273 b=2,235 d=2,231	b=2,270 d=2,261 c=2,429	a=2,250 b=2,288 d=2,269 c=2,435
Indirect Tensile Strength (MPa)	a= not possible b=1,51		a=0,487
IDT Stiffness (MPa)		b=6417	b=6530
COMBINED SAMPLE	**L 12 2 b + L 12 5 b**		**L 12 2 a + L 12 7 a**
Max. density ρ_m (Mg/m^3)	b=2,424		a=2,451
Other testing			DSR
X-Ray Scanning	NO	NO	NO
			

Location: Kehä II: Northbound direction	Lane: 11: **SMA 16 REM 2008**	Area: M

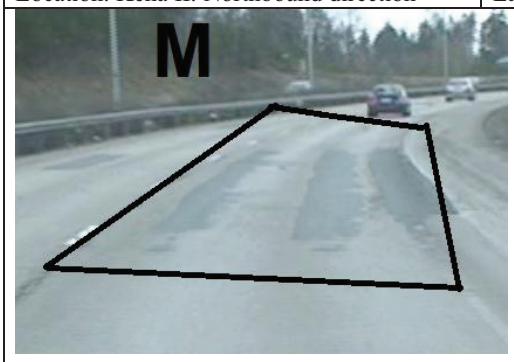

Coordinates: 60 11' 40'' N 24 44' 37'' E

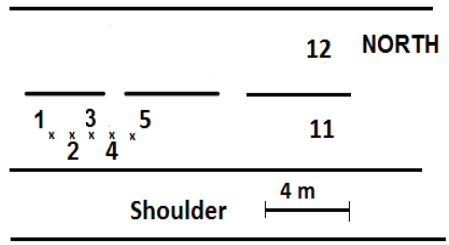

Distance between samples 1 m,
to the end of the shoulder 4,5m

Comments:
This was a bad area with several patches. It is difficult to see where the joint between the REM and SMA layers is. Layer (b) and (c) were not attached.

SAMPLES	**M 11 1 a b c**	**M 11 2 a b c**	**M 11 3 a b**	**M 11 4 a b c (NS&T)**	**M 11 5 a b c (NT)**
Thickness (mm)	a=51,91 b=31,38 c=76,86	a=55,87 b=29,09 c=89,93	a=56,13 b= 29,45	a=52,58 b=36,61 c=81,74	a=57,40 b=31,70 c=61,45
Air voids % with estim. max. density ρ_m 2,457	a=6,0 (2,438) b=7,8 (2,430) c=4,4 (2,437)	a=4,8 (2,438) b=8,3(2,430) c=3,8 (2,437)	a=5,0 (2,438) b=7,0 (2,430)	abc=6,5 (2,468)	ab=5,1 (2,437) c=3,1 (2,437)
Bulk density SSD (Mg/m^3)	a=2,291 b=2,240 c=2,330	a=2,322 b=2,228 c=2,345	a=2,317 b=2,261	abc=2,308	ab=2,314 c=2,361
ITSR (MPa)	a=1,47 b=1,08	a=2,17 b=1,39	a=1,95		
ITS (MPa)	a=4869	a=7431	a=6081		
COMBINED	**M 11 1 b + M 11 2 b**				
Max. (Mg/m^3)	b=2,430		a=2,438		
X-Ray Scanning	NO	NO	NO	YES	NO
	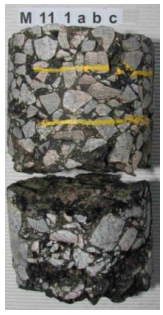				

Location: Kehä II: Northbound direction	Lane: 11: **SMA 16 REM 2008**	Area: N

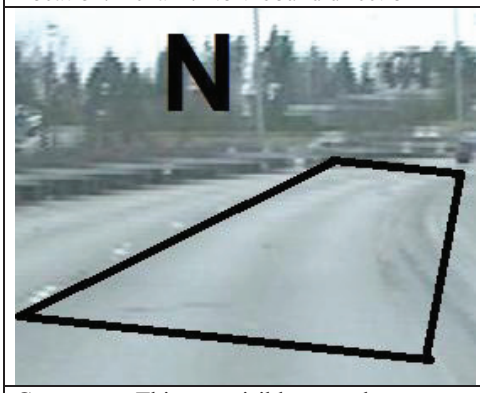

Coordinates: 60 11' 42'' N 24 44' 37'' E

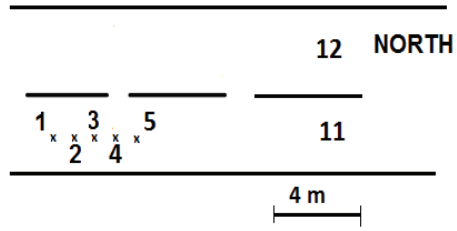

Distance between samples 1m, to the shoulder 1,5 m

Comments: This was visibly a good area.

SAMPLES	**N 11 1 a b c**	**N 11 4 a b c**	**N 11 2 a b c (NS&T)**	**N 11 3 a b c (NS&T)**	**N 11 5 a b c (NS&T)**
Thickness (mm)	a=46,81 b=53,0 c=67,73	a=49,96 b=37,64 c=77,35	a=48,09 b=41,08 c=69,41	a=54,48 b=36,23 c=67,94	a=45,46 b=42,32 c=48,56
Air voids (%)	a=2,8 (2,443) b= 7,1 (2,430) c=4,3 (2,437)	a=3,9 (2,443) b= 6,2 (2,430) c= 2,2 (2,437)	abc=5,2 (2,467)	abc=4,6 (2,467)	ab=5,3 (2,439) c=4,22,437)
Bulk density SSD (Mg/m^3)	a=2,375 b=2,257 c=2,331	a=2,347 b=2,279 c=2,384	abc=(2,339)	abc=2,335	ab=2,310 c=2,334
IT Strength (MPa)	a=2,39 b=1,93	a=2,36 b=1,91			
IT Stiffness (MPa)	a=9168	a=8699 b=5215			
Max. density ρ_m (Mg/m^3)	a=2,443				
COMBINED	**N 11 1 b + N 11 4 b**				
Max. density ρ_m (Mg/m^3)	b=2,430				
X-Ray Scanning	NO	NO	NO	YES	NO
					

Location: Kehä II: Northbound direction	Lane: 12: **SMA 16 LTA 2011**	Area:O

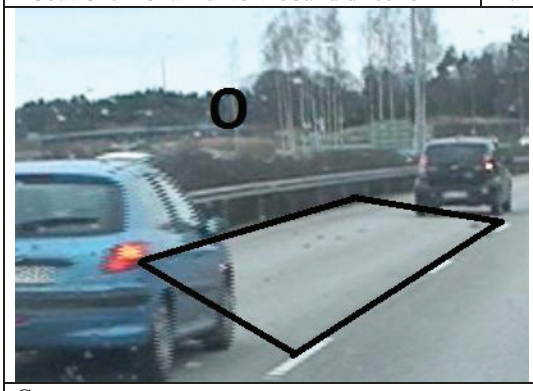

Coordinates: 60 11´22´´ N 24 44´56´´E
(same location as E but from line 1.2)

Comments:
Sample was taken on 30th of January 2012. This must be a location were road has been fixed due to perhaps base layer settlement with some fine leveling course mixture designated as (d).

SAMPLES	**O 12 1 TL a b d**
Thickness (mm)	TL=40,53 a=31,99 b=38,88 d=59,36
Air voids content %	TL=3,1
Bulk density ρ_b (Mg/m^3)	TL=2,489
Max. density ρ_m (Mg/m^3)	TL=2,569
IT Strength (MPa)	TL=1,86
IT Stiffness (MPa)	TL=4752
X-Ray Scanning	NO

Appendix B: Meteorological information

Sepänkylä	Temperature °C								Precipitation mm	
Date	hr 03	hr 06	hr 09	hr 12	hr 15	hr 18	hr 21	hr 24	Kaisaniemi	Nupuri
26.7.2007	16,9	16,6	17,7	22,2	22,1	22,8	21,6	17,1	-	-
27.7.2007	14,9	14,7	18,4	21,4	21,3	19,5	17,3	16,4	1,2	2,7
28.7.2007	15,8	13,7	16,4	18,5	18,9	18,8	16,1	13,9	-	0,1
29.7.2007	14,3	14,8	15,6	17,5	18,5	18,0	16,7	13,7	2,5	1,5
30.7.2007	12,8	12,3	14,7	15,9	15,9	16,3	13,6	13,5	20,4	23,7
31.7.2007	13,5	12,8	13,4	13,4	13,1	13,9	13,8	14,9	3,4	13,6
1.8.2007	13,8	13,8	16,2	18,6	20,2	21,2	17,5	14,7	-	-
2.8.2007	15,5	14,7	14,3	15,5	18,8	19,1	17,3	15,7	-	-
3.8.2007	13,5	13,6	15,7	18,1	19,9	19,3	16,8	12,8	-	-
	Temperature °C								Precipitation mm	
Date	hr 03	hr 06	hr 09	hr 12	hr 15	hr 18	hr 21	hr 24	Kaisaniemi	Nupuri
16.7.2008	16,0	16,8	16,6	18,5	18,8	20,0	17,3	13,6	0,1	-
17.7.2008	11,6	12,6	17,0	18,6	16,7	16,6	16,6	12,4	2,0	1,3
18.7.2008	11,2	11,1	16,6	18,5	20,3	19,8	17,1	13,2	-	-
19.7.2008	14,4	12,5	17,2	19,7	21,0	21,0	19,2	15,0	-	-
20.7.2008	12,6	12,5	17,4	20,7	20,6	19,0	15,2	15,5	0,2	0,1
21.7.2008	15,9	15,8	16,3	21,2	20,2	20,9	16,9	15,7	-	1,0
22.7.2008	15,0	15,8	17,2	18,2	17,6	17,9	17,3	15,7	0,1	10,0
23.7.2008	14,8	15,1	18,2	21,8	25,0	25,1	21,8	16,6	-	-

Appendix C: Copies of construction records.

Fly ash, Loss of Ignition manufacturer's QC reports

Höyryn lentotuhkan hehkutushäviö

Heinäkuu 2002

Pvm	Hehkutushäviö %
3.7.2002	5.9%
4.7.2002	6.1%
7.7.2002	7.0%
9.7.2002	6.8%
11.7.2002	6.7%
14.7.2002	6.8%
16.7.2002	5.0%
18.7.2002	5.0%
21.7.2002	3.5%
24.7.2002	4.0%
25.7.2002	4.3%
28.7.2002	4.3%
30.7.2002	4.8%

Elokuu 2002

Pvm	Hehkutushäviö %
4.8.2002	4,7%
8.8.2002	5,1%
11.8.2002	4,0%
13.8.2002	3,6%
15.8.2002	7,8%
18.8.2002	6,7%
22.8.2002	6,2%
25.8.2002	7,1%
27.8.2002	6,6%
29.8.2002	5.1%

Syyskuu 2002

Pvm	Hehkutushäviö %
2.9.2002	3,4%
4.9.2002	3,7%
6.9.2002	5,4%
8.9.2002	6,6%
12.9.2002	7,0%
15.9.2002	5,7%
17.9.2002	3.9%
19.9.2002	4.2%
22.9.2002	4.1%
24.9.2002	4,8 %
26.9.2002	5,8 %
29.9.2002	5.8%

Lokakuu 2002

Pvm	Hehkutushäviö %
3.10.2002	5.4 %
8.10.2002	3,2%
10.10.2002	2,8%
13.10.2002	3.0%
15.10.2002	3.5%
17.10.2002	3.5%
27.10.2002	6.3%

Marraskuu 2002

Pvm	Hehkutushäviö %
3.11.2002	4.4 %
7.11.2002	6.9%
10.11.2002	6.9%
13.11.2002	6.7%
14.11.2002	5.9%
17.11.2002	5,4%

Mineral filler QC report from asphalt plant

HIENOAINESTUTKIMUSSELOSTE

Tieliikelaitos
Konsultointi

Päivämäärä 12.7. 2002

Laboratorio Nrc 295 / 2002

TILAAJA	
TIEL. Asfalttiasema, Maantiekylä	
NÄYTTEEN OTTOPAIKKA	
Asf.asema, Maantiekylä	
NÄYTTEEN OTTOAIKA	NÄYTTEEN OTTAJA
9.7.2002	ei ilmoitettu
NÄYTTEEN TIEDOT	
Täytejauhe KF, valmistaja/myyjä Lohja, toimituspaikka Tytyri, kuormakirjan nro TY 023 08972	

Koe		Kokeen tunnus 1			VAATIMUKSET Min	Max
Vesipitoisuus, m-%	PANK 2109	0,1				1,0
Rakeisuus, seulan 2 mm läpäisy-%	SFS-EN 933-1	100			100	
Rakeisuus, seulan 0,125 mm läpäisy-%	SFS-EN 933-1	94,5			85	100
Rakeisuus, seulan 0,063 mm läpäisy-%	SFS-EN 933-1	78,1			70	100
Liukoisuus suolahappoon, %	PANK 2405	93,7			75	

LAUSUNTO:

Allekirjoitus

Laborantti Lea Korte

Laborantti Leena Nieminen

JAKELU:

Konsultointi, Geopalvelut
Helsingin laboratorio

KAYNTIOSOITE
Opastinsilta 12 A

POSTIOSOITE
PL 157 00521 HELSINKI

PUHELIN
020 444 2136

TELEFAX
020 444 2019

Cellulose Fiber Manufacturer's data sheet

Data sheet

GRADE
80premium

VIATOP®

VIATOP® 80 premium is a granulated blend of 80 % by weight ARBOCEL® ZZ 8 - 1 and 20 % by weight bitumen.

Characteristics of the Granulate

grey, cylindrical pellets

Content ARBOCEL® ZZ 8 - 1	79 - 84 %
Average pellet length	2 - 8 mm
Average pellet thickness	5 ± 1 mm
Bulk density	450 ± 50 g/l
Sieve analysis: finer than 4,5 mm	max. 7 %

Non-toxic and physiologically safe.

Characteristics of ARBOCEL® ZZ 8 - 1

grey, fine fibrilled and long-fibred cellulose.

Basic raw material	technical raw cellulose
Cellulose content	80 ± 5 %
pH-value (5 g/100 ml)	7,5 +/- 1
Average fibre length	1100 µm
Average fibre thickness	45 µm

Characteristics of the bitumen used

Road construction bitumen according to DIN 1995.

Needle penetration (according to DIN 52 010) at 25 °C in 1/10 mm	35 - 50
Softening point (ring and ball, according to DIN 52 011) in °C	54 - 59

JRS

J. RETTENMAIER & SÖHNE GMBH + CO
Fibers designed by Nature
Holzmuehle 1
D-73494 Rosenberg

Telephone: 0 79 67/1 52-0
Telefax: 0 79 67/ 1 52 - 222

0301

Bitumen manufacturer's QC reports

BITV1500 ANALYYSIT 01.09. - 30.09. (Naantali)

Fortum

Tämän laatutodistuksen tuoteominaisuuksia kuvaavat arvot sitovat toimittajaa toimitusvarastonsa lastausvarren ulostuloon asti. Mikäli ostaja seostaa tai lisää toimittajan tuotteeseen kolmannen osapuolen valmistamia tuotteita tai aineita, toimittaja ei vastaa seoksen laadusta eikä tätä laatutodistusta voida käyttää seoksen laadun kuvaajana.

	Säiliö: Näyte:	06.09. Valmistus Myynti	11.09. Valmistus Myynti	18.09. Valmistus Myynti	Laatu-vaatimus
Viskositeetti 60 °C	mm²/s	1730	1300	1600	1000...2000
Leimahduspiste,PMcc	°C	233	234	239	min. 200
Ohutkalvokoe					
Massan muutos	m-%	-0,12	-0,11	-0,11	min. -0,60

Analyysit /kuu 2007

Viskositeettisuhde		1,8	1,5	1,7	maks. 3,0

	Säiliö: Näyte:	24.09. Valmistus Myynti	Laatu-vaatimus
Viskositeetti 60 °C	mm²/s	1400	1000...2000
Leimahduspiste,PMcc	°C	232	min. 200
Ohutkalvokoe			
Massan muutos	m-%	-0,15	min. -0,60
Viskositeettisuhde		1,4	maks. 3,0

BITV1500 ANALYYSIT 01.10. - 24.10. (Naantali)

Fortum

Tämän laatutodistuksen tuoteominaisuuksia kuvaavat arvot sitovat toimittajaa toimitusvarastonsa lastausvarren ulostuloon asti. Mikäli ostaja seostaa tai lisää toimittajan tuotteeseen kolmannen osapuolen valmistamia tuotteita tai aineita, toimittaja ei vastaa seoksen laadusta eikä tätä laatutodistusta voida käyttää seoksen laadun kuvaajana.

	Säiliö: Näyte:	06.10. Valmistus Myynti	09.10. Valmistus Myynti	12.10. Jakelu Tarkistus	Laatu-vaatimus
Viskositeetti 60 °C	mm²/s	1500	1760	1570	1000...2000
Leimahduspiste,PMcc	°C	225	242		min. 200
Ohutkalvokoe					
Massan muutos	m-%	-0,13	-0,08		min. -0,60
Viskositeettisuhde		1,4	1,5		maks. 3,0

	Säiliö: Näyte:	22.10. Jakelu Tarkistus	Laatu-vaatimus
Viskositeetti 60 °C	mm²/s	1800	1000...2000
Leimahduspiste,PMcc	°C		min. 200
Ohutkalvokoe			
Massan muutos	m-%		min. -0,60
Viskositeettisuhde			maks. 3,0

BIT65 ANALYYSIT 30.09. - 24.10. (Porvoo)

Fortum

Tämän laatutodistuksen tuoteominaisuuksia kuvaavat arvot sitovat toimittajaa toimitusvarastonsa lastausvarren ulostuloon asti. Mikäli ostaja seostaa tai lisää toimittajan tuotteeseen kolmannen osapuolen valmistamia tuotteita tai aineita, toimittaja ei vastaa seoksen laadusta eikä tätä laatutodistusta voida käyttää seoksen laadun kuvaajana.

VTT Mix Design Report and JMF, Page 1

VTT RAKENNUS- JA YHDYSKUNTATEKNIIKKA

TESTAUSSELOSTE N:o RTE 1558/02

Tulokset

1. Kiviainekset ja muut raaka-aineet

	Tiheys	*Rakeisuus*
KaM Koskenkylä 0/2	2700	liite 1
KaM Koskenkylä 5/8	2690	liite 1
KaM Koskenkylä 8/16	2680	liite 1
Täytejauhe, kf Sipoo (VTT)	2770	liite 1
Bitumi B 70/100, Fortum (VTT)		
Kuitu EKI 12 (VTT)		

2. Suhteitukset

Koekappaleet (Ø=100 mm, h=100 mm) valmistettiin ICT-kierto-tiivistimellä (150RB-204) eri sideainepitoisuuksin. Optimisideainemäärällä (6,1 %) tiivistettiin koelaatat, joista porattiin näytteet eri testeihin: creep-koe (100/100 & 100/150, SRK ja vedenkestävyys). Koekappaleiden ominaisuudet ovat taulukossa 1:

		SMA 16	Menetelmä	Ohje
ICT-suhteitus:				
Bitumi-%, opt	p-%	6,1		
Pääll.tiheys	kg/m^3	2377	PANK 4112	
Massan tiheys	kg/m^3	2446	PANK 4108	
Tyhjätila TT	til-%	2,8	PANK 4114	2 - 5
KAT	til-%	17	"	16-20
Täyttöaste	til-%	83	"	80-90(85)
Rakeisuus	liite	1		
Laatta ja sen toiminnalliset ominaisuudet:				
Bit-%	p-%	6,1		
Pääll.tiheys	kg/m^3	2380	PANK 4112	
TT	%	2,7	PANK 4114	
KAT	%	17	"	
TA	%	84	"	
Creep (100/100)	%	3,0	PANK 4208	≤ 3,5 (II lk)
Creep (100/150)	%	1,8	PANK 4208(EN)	≤ 2,0 (I lk)*
SRK	cm^3	28	PANK 4209	≤ 35 (II lk)
Vedenkestävyys				
- hvl-ilma	kN/m^2	1660		
- hvl-vesi	kN/m^2	1700		
- kerroin	%	102	PANK 4301	≥ 80

VTT YHDYSKUNTATEKNIIKKA

LIITE 1
RTE 1558/02

Tilaaja: Asfalttiasema/Böckerman
Kohde: UP
Massa: SMA 16/tiivis versio 3
Sideaine: B-80 6,1 %
Täytejauhe: KF Sipoo
Lisäaineet: Irtokuitu EKI 12 0,33 % 0,3

Kiviaines: Koskenkylä 2000
Muuta: hienonema ei mukana
Massan tiheys: 2447 kg/m³

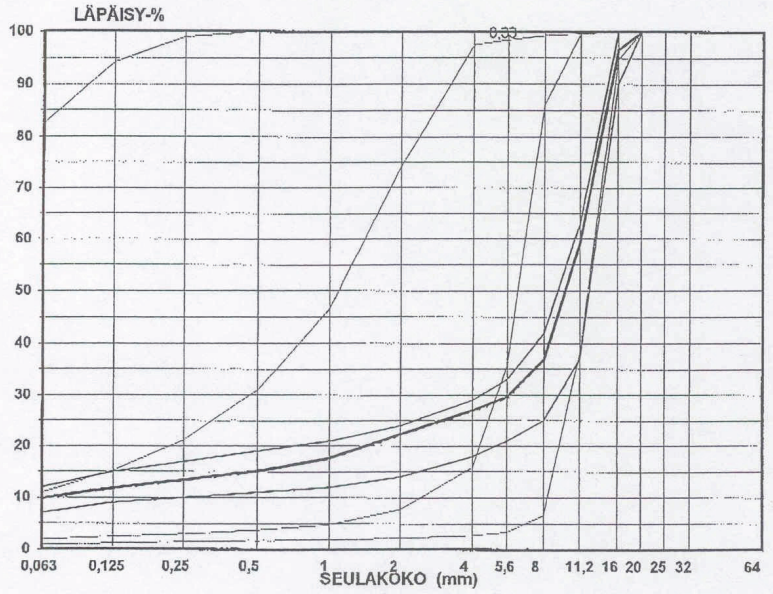

	Tiheydet:	2692	2770	2700		2690		2680
	Seososuudet:	100,0 %	9,0 %	15,0 %	0,0 %	10,0 %	0,0 %	66,0 %
Seula	Alaraja	Yläraja	Seos	kf	0-2		5-8		8-16
0,063	7	12	9,9	82,6	10,9		1,9		0,9
0,125	9	15	11,8	94,2	15,2		2,5		1,2
0,25	10	17	13,4	99	21,2		3		1,5
0,5	11	19	15,1	100	31		3,7		1,7
1	12	21	17,7	100	46,7		4,8		1,9
2	14	24	22,4	100	74,2		7,7		2,2
4	18	29	27,0	100	97,5		15,8		2,7
5,6	21	33	29,6	100	98,5		35,9		3,4
8	25	42	36,8	100	99,3		86,2		6,5
11,2	37	63	59,1	100	99,7		99,7		38,2
16	90	100	96,5	100	100		100		94,7
20	100	100	100,0	100	100		100		100
25			100,0	100	100		100		100
32			100,0	100	100		100		100

böckalit2002sma1 6u 14.5.2002

QC report for DOR measurements of air voids content

Laatuinsinöörit Oy

ARVONI

Proje : 501KO 09/501 KEHÄ II

Massan tilavuuspaino : 2.456

Asfaltti/työtapa : EA/SMA 16

Ylitysraja	:	6.00
Alitusraja	:	0.00
Keskihajontaraja	:	3.00
Matkalta	:	Koko projekti
Metriä/näyte	:	5
Näytteitä	:	4448 kpl
Linja (0=kaikki	:	0

Ylitykset, kpl	:	30
Ylitykset, summa	:	22.62
Ylitysprosentti	:	0.08
Taulukon lähimmät:		0- 1 ylitys%
Taulukon lähimmät:		0.000- 0.00 muutos%
Arvonmuutos, ylitys:		0.0000 %

Alitukset, kpl	:	36
Alitukset, summa	:	29.828
Alitusprosentti	:	0.00
Taulukon lähimmät:		0- 1 alitus%
Taulukon lähimmät:		0.000- 0.00 muutos%
Arvonmuutos, alitus:		0.0000 %

Keskiarvo(tyhjätila)	:	2.71
Keskihajonta(tyhjätila)	:	2.42
Taulukon lähimmät	:	2- 2 hajonta
Taulukon lähimmät	:	0.15- 0.10 muutos%
Arvonmuutos hajonnan mukaan	:	0.14 %

Asphalt plant mix quality QC results

Tielaitos **Näytetutkimustulokset**

SMA16	Luokka B Seulonta Koneasemalta 1 Maantiekylä/ARA 1 2 3 4 5 6 7 8 9 10 11 12 13 14 15 16 17 18 19 20 21 22 23 24 25 26 27 28 29 30 31 32 33 34 35 36 37 38 39 40 41 42 43 44 45 46 47 48 49 50 51 52 53 54 55																	
SMA16	Side-%	Täyte-%	Vesi-%	0.063	0.125	0.25	0.5	1	2	4	5.6	8	11.2	16	22.4	31.5	40	50	64
Kpl	71			71	71	71	71	71	71	71	71	71	71	71	71	71	71	71	71
Keskiarvo	5.97			9.91	12.25	14.27	15.79	17.67	20.45	22.65	24.08	29.77	56.03	95.09	100.00	100.00	100.00	100.00	100.00
Keskihajonta	0.11			0.51	0.56	0.58	0.64	0.82	1.24	1.52	1.47	1.85	3.65	1.71	0.00	0.00	0.00	0.00	0.00
Poikkeamat Kpl	0			0	0	0	0	0	0	0	0	0	0	0	0	0	0	0	0
Poikkeamat %	0.00			0.00	0.00	0.00	0.00	0.00	0.00	0.00	0.00	0.00	0.00	0.00	0.00	0.00	0.00	0.00	0.00
TMP-%	0.63			0.01	0.00	0.00	0.00	0.00	0.01	0.00	0.00	0.50	0.00	0.00	0.00	0.00	0.00	0.00	0.00
Alaohjearvo	5.70			8.00			12.00		15.00			25.00							
Alitus kpl	0			0	0	0	0	0	0	0	0	0	0	0	0	0	0	0	0
Alitus %	0.00			0.00	0.00	0.00	0.00	0.00	0.00	0.00	0.00	0.00	0.00	0.00	0.00	0.00	0.00	0.00	0.00
Yläohjearvo	6.50			12.00			20.00		25.00			37.00							
Ylitys kpl	0			0	0	0	0	0	0	0	0	0	0	0	0	0	0	0	0
Ylitys %	0.00			0.00	0.00	0.00	0.00	0.00	0.00	0.00	0.00	0.00	0.00	0.00	0.00	0.00	0.00	0.00	0.00
Lask. ohje	6.10			10.00			16.00		20.00			31.00							
Alku kpl																			
Ohjearvo	6.10			10.00			16.00		20.00			31.00							

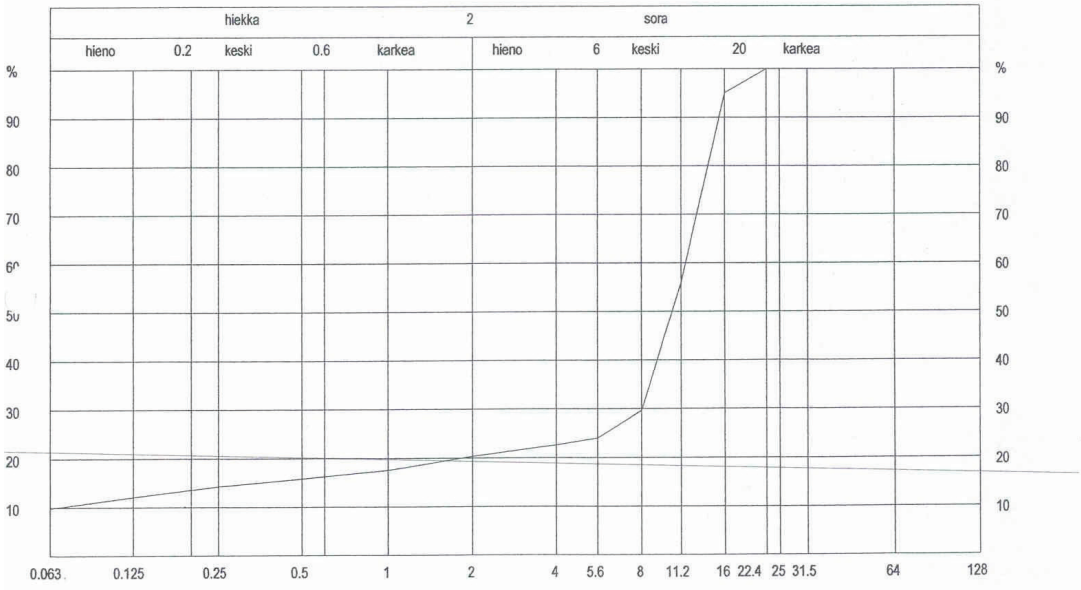

8.11-02 S.U

This research has been conducted in collaboration with Liikennevirasto (Finnish Transport Agency).

Aalto-ST 18/2013

ISBN 978-952-60-5265-6 (pdf)
ISSN-L 1799-4896
ISSN 1799-4896
ISSN 1799-490X (pdf)

Aalto University
School of Engineering
Department of Civil and Environmental Engineering
www.aalto.fi

BUSINESS +
ECONOMY

ART +
DESIGN +
ARCHITECTURE

**SCIENCE +
TECHNOLOGY**

CROSSOVER

DOCTORAL
DISSERTATIONS